Thesis

Correlation of lipid signatures with multidrug resistance in *CIC::DUX4* sarcoma based on a novel patient-derived model

submitted by

Florian Zemljic

in partial fulfillment of the requirements for the degree of

Doktor der gesamten Heilkunde

(Dr. med. Univ.)

at the

Medical University of Graz

Executed at the

Department of Biomedical Research

Under the Supervision of

Beate Rinner, Assoz. Prof. Priv.-Doz. Mag. Dr.

And at the

Diagnostic and Research Institute of Pathology

Bernadette Liegl-Atzwanger, Univ.-Prof. Priv.-Doz. Dr.med.univ.

Graz, am 07.08.2023

Declaration of Academic Integrity

I hereby confirm that the present diploma thesis is the result of my own independent scholarly work. I also confirm that in all cases, where material from the work of others (in books, articles, essays, dissertations, and on the internet) is acknowledged, quotations and paraphrases are clearly indicated. No material other than that cited in the reference list has been used. I have read and understood the Medical University's regulations and procedures concerning plagiarism.

Graz, am 07.08.2023 *Florian Zemljic eh.*

Acknowledgements

I would like to say thank you to my supervisor Assoz. Prof. Priv.-Doz. Mag. Dr. Beate Rinner, Vejzovic, Djenana MSc, BSc, Silke Schrom MSc, BSc and Thomas Hebesberger, MSc, BSc from the Core Facility Alternative Biomodels and Preclinical Imaging and Univ.-Prof. Priv.-Doz. Dr.med.univ. Bernadette Liegl-Atzwanger, D&R Institute of Pathology for supporting me, providing help and bringing ideas for this diploma thesis.
Of course, I thank my parents for the support through my whole study and my brother.
Also, thanks to my friends and all the other, who supported me, and I have forgot to mention.

This thesis was created with the financial support of the scientific funding provided by the Department of Culture of the City of Graz.

Mit freundlicher
Unterstützung der Stadt Graz
GRAZ

Zusammenfassung

Das *CIC::DUX4*-Sarkom ist eine seltene Art von Sarkomen, die durch eine chromosomale Translokation gekennzeichnet ist, bei der die Gene CIC und DUX4 fusionieren. Die Untersuchung des Lipidstoffwechsels in *CIC::DUX4*-Sarkomen kann wertvolle Erkenntnisse über die metabolischen Veränderungen liefern, die der Pathogenese dieser bösartigen Erkrankung zugrunde liegen und möglicherweise die Entwicklung zielgerichteter therapeutischer Ansätze unterstützen. In dieser Studie hatten wir das Ziel, das Lipidprofil der *CIC::DUX4*-Sarkom-Zelllinie MUG CIDUS zu charakterisieren und mit der EWING Sarkom Referenzzelllinie MHH-ES-1 (*EWSR1::FLI1* Fusion) zu vergleichen.

Die Lipidom-Analyse wurde unter Verwendung massenspektrometrischer Techniken an Lipidextrakten beider Zelllinien durchgeführt. Eine umfassende Profilerstellung ermöglichte die Identifizierung und Quantifizierung verschiedener Lipidarten, einschließlich Phospholipiden, Sphingolipiden und Cholesterin.

Die Ergebnisse zeigten signifikante Unterschiede in den Lipidprofilen zwischen der *CIC::DUX4*-Sarkom-Zelllinie MUG CIDUS und der Referenzzelllinie MHH-ES-1. Es wurden Veränderungen in den Spiegeln bestimmter Lipidarten beobachtet, was auf eine Dysregulation der Lipidstoffwechselwege im Zusammenhang mit dem *CIC::DUX4*-Fusionsgen hindeuten kann. Diese Ergebnisse liefern Hinweise auf charakteristische Lipidmuster im *CIC::DUX4*-Sarkom, die möglicherweise zum Verständnis seiner einzigartigen Pathogenese beitragen können.

Darüber hinaus ermöglichte der Vergleich der Analysen die Identifizierung von Lipidmarkern, die die *CIC::DUX4*-Sarkom-Zelllinie von der Referenzzelllinie unterscheiden. Diese Lipidmarker könnten potenzielle Ziele für die Entwicklung therapeutischer Strategien sein, die speziell darauf abzielen, den Lipidstoffwechsel im *CIC::DUX4*-Sarkom zu stören.

Zusammenfassend liefert diese Studie neue Erkenntnisse zum Lipidprofil der *CIC::DUX4*-Sarkom-Zelllinie MUG CIDUS und hebt signifikante Unterschiede im Vergleich zur Referenzzelllinie MHH-ES-1 hervor. Diese Ergebnisse tragen zum Verständnis der metabolischen Veränderungen bei, die mit dem *CIC::DUX4*-Sarkom verbunden sind und können wichtige Implikationen für die Entwicklung zielgerichteter Therapien haben. Weitere Untersuchungen zur funktionellen Bedeutung der identifizierten Lipidarten und ihrer Rolle in der Pathogenese des *CIC::DUX4*-Sarkoms sind erforderlich.

Abstract

CIC::DUX4 sarcoma is a rare subtype of sarcoma distinguished by a recurring chromosomal translocation, which leads to the fusion of the CIC and DUX4 genes. The study of lipid metabolism in *CIC::DUX4* sarcomas can provide valuable insights into the metabolic alterations underlying the pathogenesis of this malignancy and potentially guide the development of targeted therapeutic approaches. In this study, we aimed to characterize the lipid profile of the *CIC::DUX4* sarcoma cell line MUG CIDUS and compare it with the reference EWING sarcoma cell line MHH-ES-1 (*EWSR1::FLI1* fusion).

Lipidomic analysis was performed using mass spectrometry-based techniques on lipid extracts obtained from both cell lines. Comprehensive profiling allowed the identification and quantification of diverse lipid species, including phospholipids, sphingolipids, and cholesterol. The results revealed significant differences in the lipid profiles between the *CIC::DUX4* sarcoma cell line MUG CIDUS and the reference cell line MHH-ES-1. Specifically, alterations were observed in the levels of specific lipid species, suggesting dysregulation in lipid metabolism pathways associated with the *CIC::DUX4* fusion gene. These findings provide evidence for distinct lipid signatures in *CIC::DUX4* sarcoma, potentially contributing to the understanding of its unique pathogenesis.

Furthermore, the comparative analysis allowed for the identification of lipid markers that distinguish the *CIC::DUX4* sarcoma cell line from the reference cell line. These lipid markers have the potential to be utilized as targets for the creation of therapeutic approaches, specifically focused on interfering with lipid metabolism in *CIC::DUX4* sarcoma.

In conclusion, this study provides novel insights into the lipid profile of the *CIC::DUX4* sarcoma cell line MUG CIDUS, highlighting significant differences compared to the reference cell line MHH-ES-1. Further investigation into the functional significance of the identified lipid species and their role in the pathogenesis of *CIC::DUX4* sarcoma is necessary.

Table of Contents

Abbreviations

CDS	CIC-DUX4 Sarcoma
CER	Ceramide
CHOL	Cholesterin
CIC	Capicua Transcriptional Repressor
CT	Computer Tomographie
DNA	Desoxyribonuclein Acid
DUX4	Double Homeobox 4
ES	Ewing Sarcoma
FA	Fatty Acid
FBS	Fetal Bovines Serum
FIH	Factor Inhibiting Hypoxia Induceable Factor
FSHD	Facioscapulohumeral Muscular Dystrophy
GBM	Glioblastoma Multiforme
HIF	Hypoxia Induceable Factor
HRE	Hypoxia Responsive Elements
LPO	Lipid Peroxidation
m	Mili
MAPK	Mitogen Activated Protein Kinase
MDR	Multi Drug Resistant
ml	Mililiter
n	Nano
PBS	Phosphate Buffered System
PC	Phosphatitylcholin
PE	Phosphatitylethylenamin
P-gp	P-Glucoprotein
PS	Phosphatitylserin
PUFA	Polyunsaturated Fatty Acids
pVHL	Van Hippel Lindau Tumour Supressor Protein
RNA	Ribonucleinacid
ROS	Reactive Oxygen Species
RTK	Receptor Tyrosin Kinase
SFA	Saturaturated Fatty Acids
SM	Sphingomyelin
TG	Triglyceride
WHO	World Health Organisation
ZMF	Center for Medical Research
µ	Mikro
µl	Mikroliter
µm	Micrometer

Table of figure and tables

1. Introduction

1.1 Soft Tissue Sarcoma (STS)

Sarcomas are a diverse group of tumors that arise from mesenchymal tissues such as bone, muscle, cartilage, and other connective tissues (1) (Figure 1). The heterogeneity of these tumors is evident in the identification of over 100 different subtypes, which differ in their pathology, clinical presentation, molecular characteristics and response to treatment (2). Soft tissue sarcoma (STS) account for 80% of sarcomas, while bone sarcomas and gastrointestinal stromal tumors (GIST) account for 15% and 5%, respectively (3,4). Despite being relatively uncommon, sarcomas can be life threatening and are responsible for a significant loss of years of life, especially in childhood cancer cases (5). The global incidence of STS is approximately 3-4/100,000 persons annually, comprising 1% of all solid malignant tumors in adults and over 20% of pediatric cancers (5,6). It is possible that the incidence of sarcomas is lower than expected because those arising in organs with parenchyma are often attributed to the affected organs themselves rather than to the adjacent connective or supportive tissue (7). Sarcoma management presents significant challenges in clinical practice due to the difficulty in distinguishing them from other cancers, delayed diagnosis resulting from the lack of symptoms, their diverse nature, highly aggressive behavior, and poor response to available therapies. According to the National Sarcoma Survey 2020, conducted by Sarcoma UK in conjunction with Quality Health, a substantial number of the asked 1117 patients (23%) commenced treatment for an unrelated illness before being diagnosed with sarcoma (8). An additional study by Raut et al. found that as many as 25% of sarcomas received conflicting histopathological diagnoses, and over half had significant clinical implications on their management with delayed referrals to sarcoma specialists due to the absence of signs and symptoms (9-11). The effectiveness of conventional treatments such as surgery, radiation and chemotherapy varies greatly due to the heterogeneity of different sarcoma subtypes. Only surgery combined with pre- or post-operative therapies has shown promising results for localized sarcomas (12). However, metastatic sarcomas respond poorly to radiation and chemotherapy, leading to high recurrence rates and low survival rates (12). While a molecular targeted approach to treatment is being explored, the molecular mechanisms behind sarcoma cell transformation are not yet fully understood.

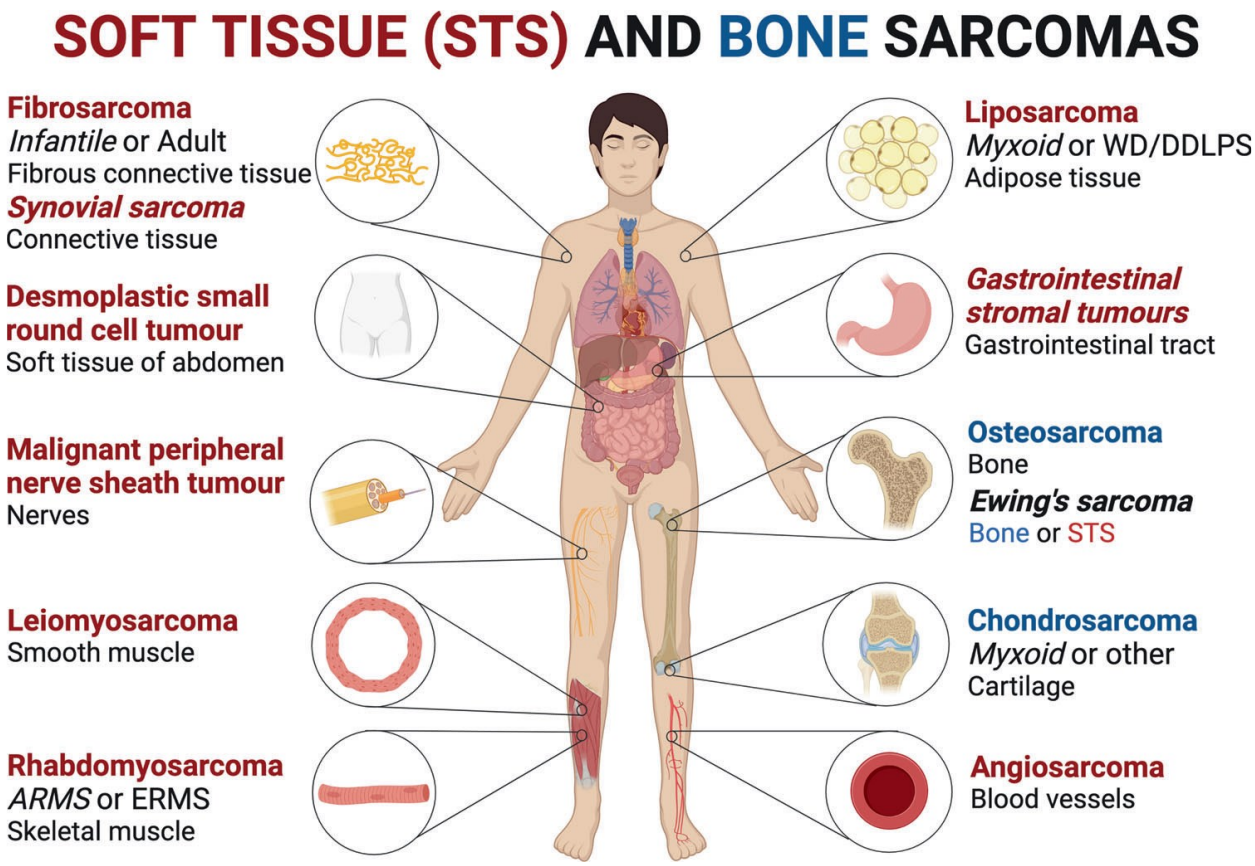

Figure 1 Various types of soft tissue and bone sarcomas (Damerell et. al. Molecular mechanisms underpinning sarcomas and implications for current and future therapy, Fig.1)
Soft tissue sarcoma can manifest in a wide variety of regions.

Sarcomagenesis is driven by fusion oncoproteins and/or mutations which activate oncogenes or disable tumor suppressors. Simple karyotypes, found in 15-20% of sarcomas, are caused by chromosomal translocations that create oncogenic fusion proteins (13). Complex karyotypes are associated with various genetic and chromosomal abnormalities, including mutation and amplification (14-16). The exact origin of sarcomas is not yet fully understood, however recent research suggests that mesenchymal stem cells (MSC) may be responsible for initiating these tumors (17,18). MSCs are a versatile type of stromal/stem cell present in various human tissues and can differentiate into different cell types, including chondrocytes, adipocytes, osteocytes, skeletal myoblasts, neural cells, and fibroblasts. Sarcomas are classified based on their similarity to a particular tissue type and lineage of cells. Two theories have been proposed for the development of sarcomas (Figure 2) - one suggests that they arise from primitive MSCs that

acquire mutations, while the other theory proposes that mutations occur in progenitor cells at different stages of differentiation, leading to a block of terminally differentiated cells and the tumor development (17). Further study is needed to fully understand the genetic alterations in sarcoma development.

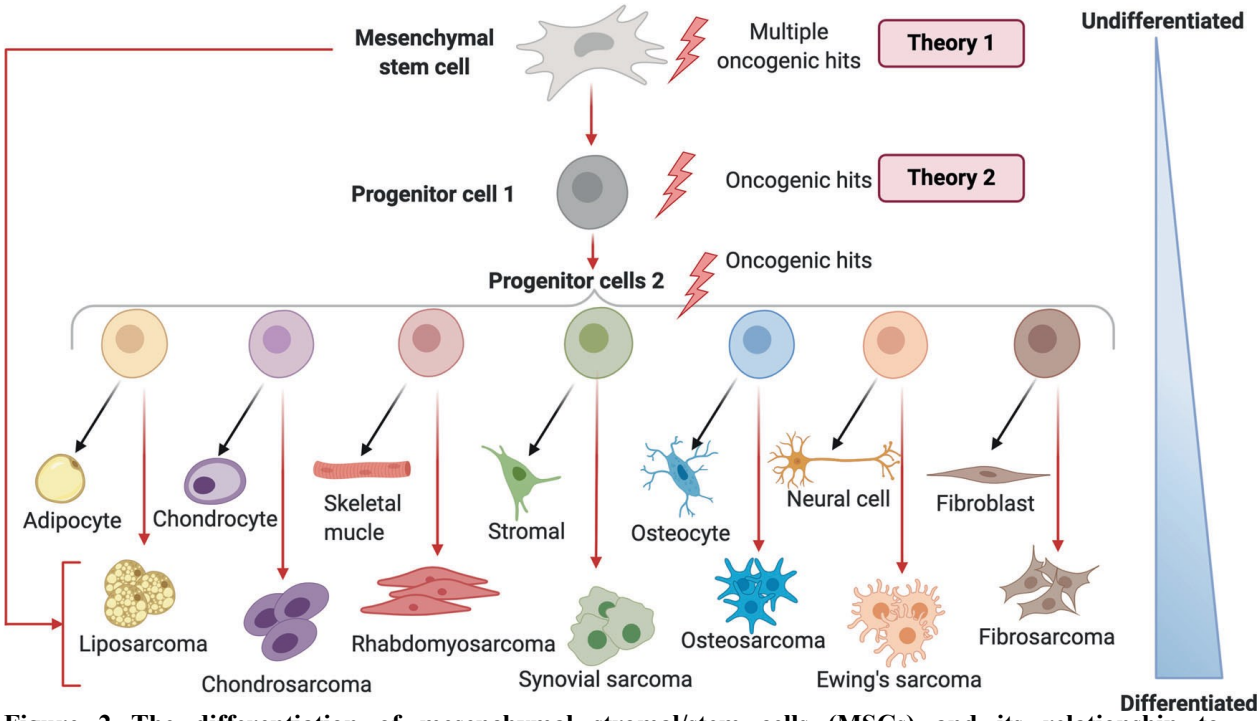

Figure 2 The differentiation of mesenchymal stromal/stem cells (MSCs) and its relationship to sarcomagenesis. (Damerell et al. Molecular mechanisms underpinning sarcomas and implications for current and future therapy Fig. 6)
Variety of cells, derived from one stem cell. This explains, why sarcoma can appear in different kinds of connective tissue. There are some theories, at which level of differentiation the malignant transformation takes place. In some cases, Ewing sarcomas can show a neural differentiation (19).

1.2 Ewing sarcoma and EWSR1-non-ETS fusion round cell sarcomas

Ewing sarcoma is a rare type of soft tissue sarcoma that accounts for less than 1%. It typically affects the metaphysis of long bones, with around 80% of cases occurring in the first and second decades of life (20). While it can manifest in adults as well, in this particular context, it tends to arise within the deep soft tissues of the paravertebral region, as well as the proximal segments of both, the upper and lower extremities (21). Ewing sarcoma can also appear in visceral locations such as the kidney (22), pancreas (23), and meninges (24), and as a primary cutaneous lesion (25). In most cases, Ewing sarcoma (ES) is characterized by the fusion of the EWSR1 gene, which belongs to the FET family of genes containing an RNA binding domain (26), with the FLI1 gene on chromosome 11q24. FLI1 is a member of the ETS family of transcription

factors (27). Other fusion transcripts involving EWSR1 or FUS with members of the ETS family (such as ERG, ETV1, ETV4, and FEV) have also been observed in ES (11-14) EWSR1 and FUS are functionally interchangeable. Routine detection of these genetic abnormalities has improved diagnostic accuracy (28). Currently, the 5-year overall survival rate for localized Ewing sarcoma is approximately 70 to 82% (29), but it drops to around 30% in cases where the cancer has metastasized (30). The prognosis for extra skeletal Ewing sarcoma remains poor, but the use of multimodal therapy – including surgical resection, radiation therapy, and chemotherapy – has led to an increase in long-term survival rates from less than 10% to around 30-40% (30).

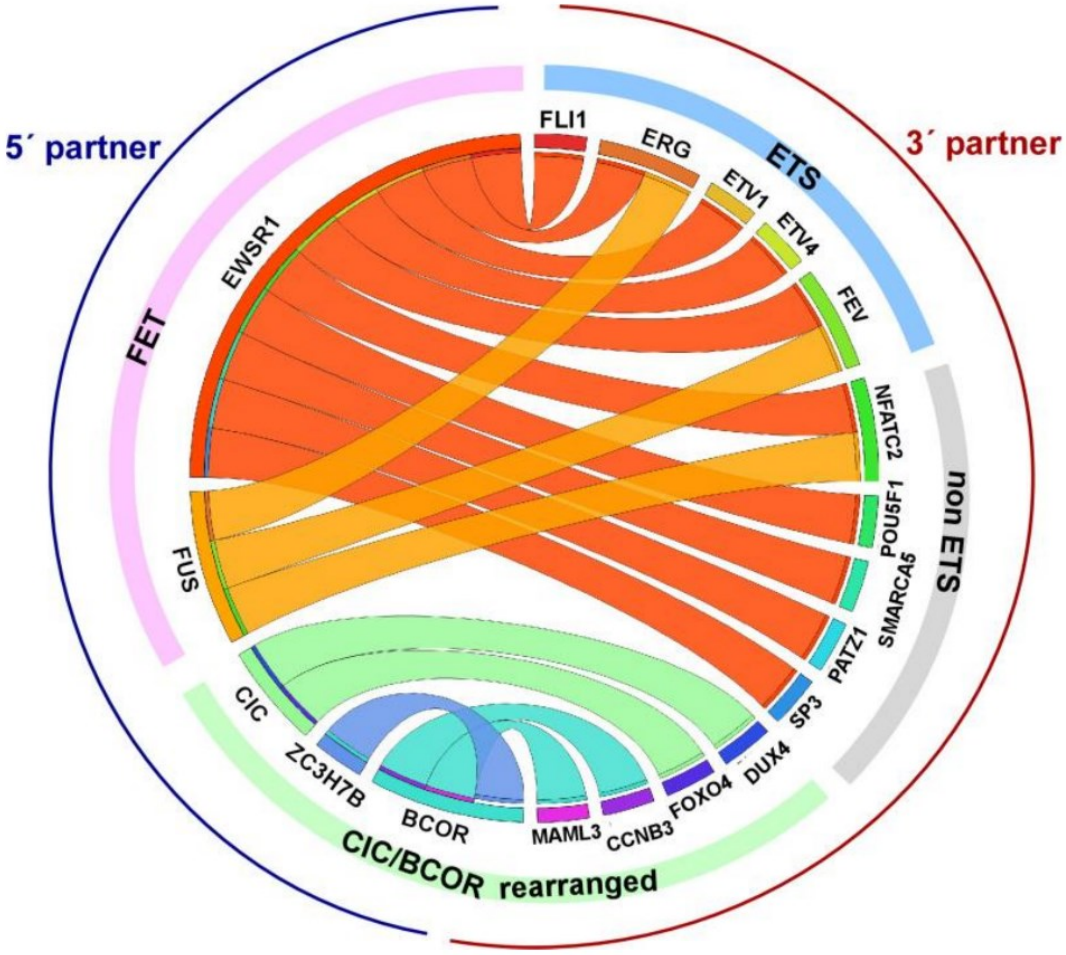

Figure 3 Combinations of Ewing, non-Ewing, CIC, and BCOR, and their partners. 5` partners in blue and 3`in red. (Salguero-Aranda et al. Breakthrough Technologies Reshape the Ewing Sarcoma Molecular Landscape, Fig. 1)
The manifold fusion partner, which can be found in ES.

Undifferentiated round cell sarcomas with rearrangements other than the mentioned gene fusions can further be divided into three main subgroups based on the gene rearrangements that underlie them: EWSR1 sarcomas that are not fused with ETS, CIC and BCOR rearranged sarcomas (31). Round cell sarcomas with rearrangements in the EWSR1 gene (or FUS) involving non-ETS fusion partners are an uncommon subset of ES (32). The genes affected by EWSR1/FUS fusions include NFATc2 (which encodes a member of the NFAT-transcription factor family or SMARCA5, a gene involved in chromatin reorganization) (33,34), and PATZ1 (35,36). *EWSR1/FUS::NFATc2* sarcomas are mainly found in the metaphysis or diaphysis of long bones (33,37), while *EWSR1::PATZ1* occur in the deep soft tissue of the chest wall and abdomen (35,36). From a clinical perspective, although complete surgery appears to provide relatively good control, about one third of patients with non-ETS-fused round cell sarcomas experience relapse or metastatic spread (35,36,38). Response to chemotherapy is typically poor, but given the rarity of these Tumors, experience is limited (39).

Pierron and colleagues identified *BCOR::CCNB3* fusion-positive sarcoma in 2012 as a new, rare member of the "Ewing-like" family of tumors (40). These sarcomas with BCOR rearrangements occur more frequently in bone than in soft tissues, representing approximately 4% of round cell sarcomas. There is a noticeable male predominance, with a peak incidence in the second decade. *BCOR::CCNB3* sarcoma more commonly affects the pelvis, lower limbs, and paraspinal region, while visceral involvement is rare (41). *BCOR::CCNB3* fusions make up 60% of BCOR gene alterations, resulting from a paracentric inversion on the X-chromosome and splicing the BCOR coding sequence with the CCNB3 exon 5 splice acceptor site. This creates an oncogenic fusion protein composed of full-length BCOR and the C-terminus of CCNB3, a cyclin involved in meiosis. In vitro studies indicate that this fusion protein drives proliferation in *BCOR::CCNB3* sarcoma, a rare type of round cell sarcoma that occurs more frequently in bone than in soft tissues. Recently, alternative fusion partners of BCOR have been identified, including MAML3 and ZC3H7B (42). Although *BCOR::CCNB3* sarcoma shares clinical and pathological similarities with Ewing sarcoma, gene profiling and SNP array analyses have shown that they are biologically distinct (43) and since WHO 2020 an own entity (44). Notably, patients with BCOR-rearranged sarcoma tend to have a more indolent clinical course than those with Ewing sarcoma, with longer overall survival linked to the location of the primary tumor in the extremities versus axial skeleton and soft tissues (41). As an overview, all mentioned fusions are shown in
Figure 3.

1.3 *CIC::DUX4* sarcoma

Although CIC-rearranged sarcomas are an own entity (44), they have been a target of discussion of how to treat them (29). The most common CIC-rearranged sarcoma harbours the distinct *CIC::DUX4* gene fusion, giving the name of the disease. *CIC::DUX4* sarcomas (CDS) are small round blue cell sarcomas of the connective and supporting tissues and bones (31). The five-year probability of survival without metastasis is between 42% and 49% (45). With lung metastasis, the most patients survival 1-2 years (46). According to current knowledge, CDS is treated with the same regimen as Ewing sarcomas - with a poor outcome in terms of five-year survival, although CDS has already been established as a separate entity (29). Recent literature has already shown that the median age is 32 - 35 (29,47) years, but in principle can occur at any age. The same was shown for the disease as a function of gender, which shows a slight dominance on the part of men (55%/45%) (45). The tumor is mainly diagnosed in the deep connective tissue (86%) with organ involvement being possible, but less common (48-50). Bones such as the hip bone are affected with a probability of 3% (29). The skin can also be affected (51). These sarcomas are diagnosed by using molecular methods (RNA sequencing).

As mentioned, the sarcoma is named after the fusion between the CIC and the DUX4 gene. The CIC gene translates for a transcriptional repressor, i.e. a protein that is supposed to prevent unwanted cell division or other commands that lead to transcription of DNA. Specifically, CIC (gene) is located on chromosome 19q13 (52) and its natural function is to block the pathway of receptor tyrosine kinases to protect the transcription factor from activation without the receptor being activated (53). To manage this, CIC (protein) sits on the DNA via its HMG motifs. If the receptor tyrosine kinase is activated properly, the MAPK pathway is activated, CIC is phosphorylated and binds to 14-3-3 protein and is degraded proteasomal after being excluded from the cell nucleus (54). In the process, sequences are also released which in turn slow down the MAPK pathway. This ensures that transcription only occurs via receptor activation. One can see this function as a filter that prevents activation by background noise. Many carcinomas like lung, gastric and prostate cancer have been described in which a CIC alteration is also present (Figure 5).

The fusion partner DUX4 is located on chromosome 4q35 or 10q26 (55). This is a "double homeobox" as an open reading frame in the D4Z4 locus of the chromosomes mentioned. Its task is to ensure proper axial development during embryonic development. DUX4 is considered a

transcription activator (56). After embryonic development it is epigenetically silenced except for activity in the germ cells of the testis and while HSV-1 infection (56). It is reported to act as a transcriptional activator. Initially, it has been identified in studies exploring the FSHD. Deletions in an array, related to the DUX4, lead to an aberrant expression in the skeletal muscle. This activation causes FSHD (57). Combined, this leads to a massive gain-of-function mutation with enormous malignant potential (58). This affects around~90% of the CIC gene and a small C-terminal part of DUX4 without its double homeodomain, but it includes its transactivation domain and its p300 binding site (59). CIC retains its HMG box and thus the ability to bind and activate at all binding sites of native CIC (60). For completeness, *CIC::DUX4* is not the only fusion of CIC. More rarely there are *CIC::NUTM1* (61,62) and 2 and *CIC::FOXO4* (47,63) fusions as small round blue cell sarcoma and *CIC::LEUTX* as angiosarcoma (64).

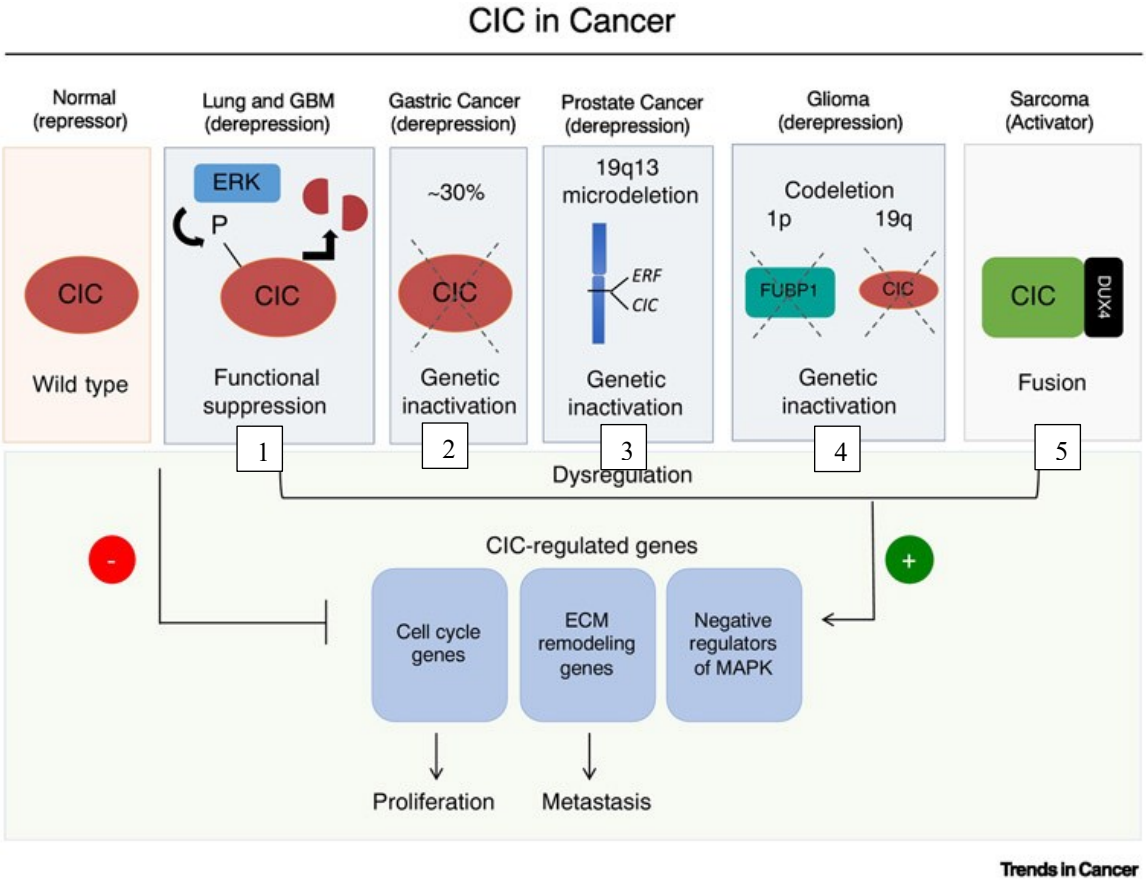

Figure 4 CIC in cancer (adapted from Ji Won Kim et al., Trends Cancer, 2021, January, page 77-86, Fig. 1) *(1) Initiation of the MAPK-ERK Pathway: This sets off a cascade, leading in the phosphorylation of CIC. This phosphorylation prompts CIC's exit from the cell nucleus with an eventual activation of genes downstream, among them ETV1 and ETV4. (2) Genetic Disruption: The loss and mutation of specific genes lead to the impairment of CIC's normal function. Resulting those downstream genes, including MET and CD44, become activated. (3) Deletion at 19q13 Locus: The removal of genetic material at the 19q13 site triggers the activation of genes further down the line, such as SOX9 and GLI1. (4) Co-Deletion of 1p19q: Oligodendroglioma demonstrates the functional*

loss of CIC through a simultaneous deletion of genetic material on chromosomes 1 and 19. This event prompts the activation of downstream genes, including IDH1 and TERT. (5) Fusion Protein CIC::DUX4:This fusion protein prompts the activation of downstream genes, including NR0B1 and MYC.

1.4 Importance of lipids in cancer and therapy

1.4.1 Membrane composition

The flexibility of cell membranes is crucial for the survival of cells in all stages, as it contributes to mechanical durability during cell division and reduces shear force, which can occur during cell division (65). Cancer cells adapt by reorganizing their plasma membranes to maintain proliferation, evade apoptosis, and resist anticancer drugs (66). This resistance is often due to decreased free diffusion of drugs through the plasma membrane (67-69), which is caused by higher levels of total cholesterol in multidrug-resistant (MDR) cells (70,71). An increased quantity of cholesterol in the membrane results in a membrane that is more inflexible and less permeable (72,73).

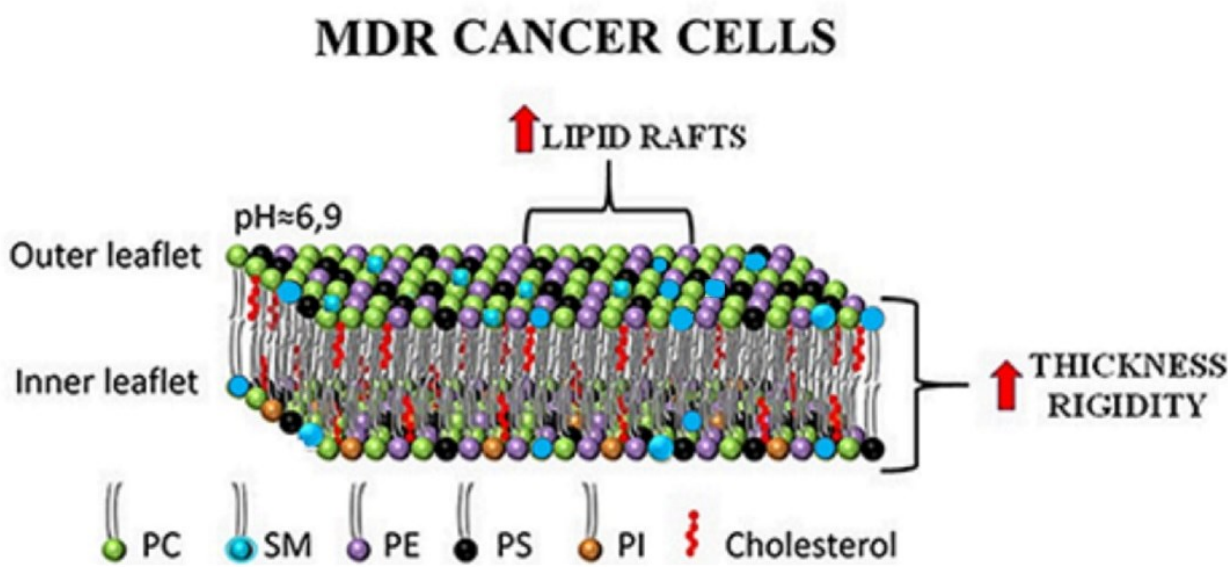

Figure 5 The membrane architecture of multi-drug resistant cancer cells (adapted from Preta et al. New Insights Into Targeting Membrane Lipids for Cancer Therapy, Fig. 1) *In cancer cells with MDR, there is an elevated concentration of PS and PE on the outer membrane surface, despite their typical localization on the inner leaflet. The abundance of CHOL in these cancer cells contributes to augmented membrane thickness and stiffness. Furthermore, MDR cancer cells showcase heightened levels of SFA chains within their membrane lipids, which has been associated with an increased presence of lipid rafts.*

MDR cells also have low ceramide levels and increased sphingomyelin (SM) synthesis, which decreases the ceramide-enriched lipid rafts involved in inducing cell death (74). Additionally,

MDR cells have increased surface expression of PS and PE, which are normally found on the inner leaflet of cell membranes (75).
The disruption of phosphatidylserine's asymmetrical distribution could be linked to a decrease in ATP-dependent phospholipid translocase activity or an increase in phospholipid scramblase activity, likely caused by elevated intracellular calcium levels (76). Alterations in ceramide (CER) metabolism have also been described as an effective drug resistance mechanism, with tumors having low CER levels due to increased sphingomyelin synthesis or prevention of CER degradation (77,78). Figure 5 illustrates the membrane lipid composition and organization in MDR cancer cells.

1.4.2 Lipid droplets

Lipid droplets (LDs) are organelles in the cytoplasm of cells that contain a core of neutral lipids, mainly triacylglycerol (TAG) and cholesteryl esters (CHOLs), surrounded by a monolayer of phospholipids and coated with structural proteins from the PAT family (79-82). The content of proteins in LDs varies depending on the cell and the conditions that stimulate their formation. The accumulation of LDs in cancer cells is a complex process that involves increased lipid uptake, de novo lipid synthesis and remodeling, as well as regulation of lipolysis. In particular, cancer cells rely heavily on fatty acid (FA) synthesis for the building blocks needed to create more complex lipids (83). The pathways that initiate lipogenesis in tumors ultimately lead to the buildup of recently created LDs (84-93). Research suggests that the mobilization of fat between stromal and cancer cells is necessary for metastasis and cancer aggressiveness. For example, in ovarian cancer, adipocytes in the omentum release cytokines and provide FAs to cancer cells, leading to increased LD formation and β-oxidation (94). This mechanism is dependent on FABP4 and the FA translocator CD36, which confers a more aggressive phenotype in cancer cells (94,95). Inhibition of CD36 reduces LD accumulation in cancer cells, limiting tumor growth and invasion both *in vitro* and *in vivo* (95). CD36 expression is also associated with poor prognosis in various types of cancer, including oral squamous cell carcinoma, lung squamous cell cancer, bladder cancer, and luminal A breast cancer (96).
The abnormal buildup of LDs is positively linked to chemoresistance in solid tumors like CRC, OvCA, and cervical cancer (97,98). In CRC cells, increased LD production facilitated by lysophosphatidylcholine acyltransferase 2 leads to resistance to 5-fluorouracil combined with

oxaliplatin, which prevents stress-induced apoptosis and reduces tumor-infiltrating CD8+ T cells (97). As a result, inhibitors of lysophosphatidylcholine acyltransferase 2 or LD biogenesis can significantly enhance tumor regression induced by dual chemotherapy and increase mice survival. Similarly, studies have shown that treating mice with ovarian and cervical tumors with carboplatin or paclitaxel, along with an inhibitor of the glycolytic enzyme PFKFB3, results in comparable outcomes by indirectly blocking LD biogenesis and lipophagy (98).

1.4.3 Cholesterol metabolism

Both, the heightened endogenous production of cholesterol and exposure to elevated circulating cholesterol levels promote cancer advancement. CHOL serves as a vital structural element of lipid rafts, which are dynamic regions of the plasma membrane that are abundant in RTKs and MDR efflux transporters (99). Doxorubicin resistance, for instance, has previously been associated with increased cholesterol levels in lipid rafts. Due to the chemical property of doxorubicin, it stays in the vicinity of cholesterol. Cholesterol surrounds P-gp, transporters that can pump substances out of the cell making more doxorubicin molecules available to these transporters reducing the intracellular concentration (100). Interestingly, treatment of MDR colorectal cancer cells with DHA and EPA was able to break this cholesterol arrangement and shift the P-GP to lower-CHOL areas, which provided them with less substrate and thus showed a higher doxorubicin concentration in the cell (101).

In vitro models of doxorubicin-induced resistance have revealed the upregulation of the mevalonate (MVA) pathway, also known as the Chol biosynthetic pathway, through Gene Ontology analysis. Upregulated genes belong to both the upstream MVA pathway, such as 3-β-hydroxy-3-β-mehyl glutaryl coenzyme A synthase 1 (HMGCS1), and the downstream MVA pathway, such as farnesyl-diphosphate farnesyltransferase 1 (FDT1), and 7-dehydrocholesterol reductase (DHCR7), which are responsible for isoprenoid and cholesterol biosynthesis (102). The elevation of both isoprenoids and cholesterol is observed in multidrug-resistant cells, including colon cancer (103), malignant pleural mesothelioma (104), non-small cell lung cancer (105), and breast cancer (106). Additionally, other proteins controlling Chol metabolism, such as Progesterone receptor membrane component 1 (PGRMC1), are overexpressed in drug-resistant cells. PGRM1 modulates Chol biosynthesis by regulating SREBP cleavage activating protein (SCAP). PGRM1 is overexpressed in doxorubicin-resistant

MES-A/DxR uterine sarcoma cells, and its knockdown has synergistic effects with the P-gp transport inhibitor verapamil, indicating that PGRM1-driven mechanisms collaborate to maintain high activity or expression of P-gp (107).

1.4.4 Lipid peroxidation

Polyunsaturated fatty acids (PUFAs) present in cell membranes can be easily oxidized by reactive oxygen species (ROS), triggering a chain of events known as LPO (108,109). This process produces various reactive aldehydes as end products that can modify cellular proteins, either by stimulating or inhibiting several transduction pathways. Among these aldehydes are 4-hydroxy-2-nonenal (HNE), 4-oxo-2-nonenal (ONE), and 4-hydroxy-2-hexenal (HHE), which have been shown to activate several pro-survival and anti-apoptotic pathways (109-123).For instance, they can activate EGFR-dependent (109) signaling and c-myc transcriptional program, promoting tumor growth and proliferation (124). They can also induce TGFβ production, making cells insensitive to growth inhibition, activate NF-κB activity, which controls cell survival, inflammation (125), and immune reactions, activate the PI3K/Akt pathway, allowing cells to escape apoptosis, and increase the expression of anti-oxidant enzymes and ABC transporters through the Nrf2/Keap1 pathway (126-128).

The collective impact of these reactive aldehydes on these pathways results in increased resistance to oxidative stress and chemotherapy (124). Moreover, as cancer cells increase in malignancy, they decrease their PUFAs content, which removes potential ROS-damaged substrates and leads to a change in the lipid profile that further enhances drug resistance (129-132). Although reactive aldehydes support the MDR phenotype, it is essential to note that the change in the lipid profile contributes to an increase in drug resistance (124). The relationships are shown in the Figure 6.

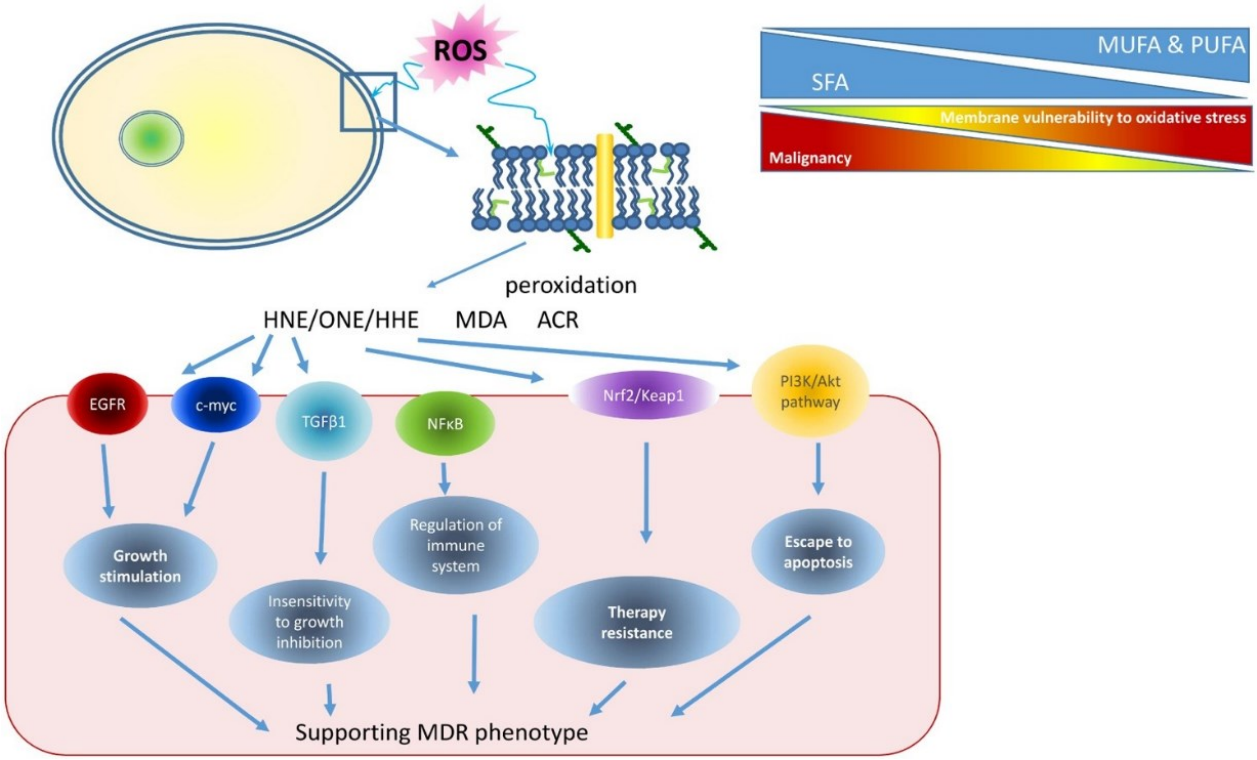

Figure 6 Lipid peroxidation (Kopecka et.al, Drug Resistance Update, March 2020, Volume 49, Fig. 2)
PUFA can easily oxidised by ROS, triggering the lipid peroxidation with a lot of end products like HNE, ONE, and HHE, MDA, ACR. ACR is also a degradation product of cyclophosphamide (ENDOXAN®). These aldehydes can stimulate a lot of pathways with a survival benefit for the cells. A switch to more stable SFA is performed by cancer cells for removing potentially substrate, which can damaged by ROS and lead to a damage of the cancer cell. This can enhance the drug resistance.

1.4.5 Ceramides

Ceramides (CER) belong to the sphingolipids and consist of a sphingosine, an unsaturated amino alcohol and a fatty acid bound to each other via an amide group. The OH group of the amino alcohol can form a bond with other groups. If this is glucose, it is called a glucosylceramide, the most common of all glycosphingolipids. CER are formed in the endoplasmic reticulum, whereas in the cis-Golgi apparatus, they become glucosylceramides by the synthase of the same name. Glucosylceramide is the starting point of over 300 types of glycerophospholipids. Conversion to sphingomyelin in the trans-Golgi is also possible (133). While CER are considered proapoptotic, meaning an increase in CER levels leads to apoptosis, this is not the case with glucosylceramides. It is possible that multidrug-resistant cells also escape apoptosis by efficiently and rapidly reducing rising CER levels induced by chemotherapeutic drugs through glucosylceramide synthase (134). Inhibition of glucosylceramide-synthase is possible and often described, portraying a potential therapeutic

target (135,136). An increase in glucosylceramides has been reported in many tumor cell lines. In addition, increased concentrations of P-gp (pumps cell toxins out of the cell under ATP consumption) protein and RNA have been documented (136,137). These observations suggest that there is a link between glucosylceramides and P-gp. As an example, the multiple increase in sensitivity to chemotherapeutic agents has been observed in a glucosylceramide synthase reduced MCF-7 breast cancer cell line (135). One possibility for inhibition is via PDMP (1-phenyl-2-decanoylamino-3-morpholino-1-propanol). With PDMP as an inhibitor of glucosylceramide (GlyCer) synthase, CER levels should be increased subsequently inducing apoptosis. However, several studies were not able to report this effect (138-140).

Resistance to doxorubicin in leukaemia cell line (K562, K562/A02) was reduced by inhibition of GlyCer synthase (133,141,142). Furthermore, there are reports of an inhibition of mTOR (mammalian target of rapamycin) in cells with GlyCer synthase inhibition. This could be an important mechanism, as high mTOR activity is considered to be unfavourable in cancer (138,143-146). mTor belongs to the protein kinases and regulates, among other things, the growth of some metabolic pathways. Because mTOR's catalytic domain is similar to that of PI3K, it belongs to the PI3K-related kinases. mTOR also forms the core component of so-called mTOR complexes (mTORC) (144,145). Dysregulation of mTOR has a potentially strong growth advantage for cancer cells. Specifically, there are descriptions that mTOR upregulates sphingolipid synthesis (133,147).

1.5 Hypoxia induced drug resistance

Cancer cells divide rapidly, outpacing the growth of blood vessels that supply them with nutrients and oxygen. As a result, the tumor is often deprived of oxygen and nutrients, creating hypoxic conditions within it. Despite this, cancer cells require significant amounts of building blocks, such as energy, proteins, and cell wall components, to sustain their rapid growth. Therefore, many tumors exhibit increased de novo synthesis of fatty acids to meet these demands (148,149). Tumor cells can promote angiogenesis by producing hypoxia-inducing factor (HIF), which has a dual effect. Firstly, it helps the tumor cells to adapt their metabolism to the hypoxic state, and secondly, it promotes the formation of new blood vessels to supply the tumor with nutrients (150).

The regulation of HIF is a straightforward process: The protein is continually synthesized, and

it contains an oxygen-dependent binding site that can be enzymatically hydroxylated under normoxia. An enzyme called HIF-PHD acts as an "oxygen sensor" and can only hydroxylate HIF under normoxic conditions. Another enzyme, with the same function is FIH (151). HIF binds to pVHL (Van Hippel Lindau tumor suppressor protein). This protein can ubiquitinate HIF and leads to a proteasomal degradation. However, under hypoxia, the HIF complex cannot be hydroxylated. It accumulates in the nucleus, activating numerous genes that affect survival under hypoxic conditions (152). This occurs through hypoxia responsive elements (HRE) in promoters of the genes (153).

In recent years, a contribution of HIF-1 to drug resistance has been observed in a wide spectrum of neoplastic cells (154-162). The significance of HIF-1 in chemosensitivity of cancer cells under normoxic conditions remains a subject of debate due to conflicting findings in available data. Some studies have failed to demonstrate any effect of HIF-1 inactivation on drug response in the presence of oxygen, such as in the case of neuroblastoma and lung adenocarcinoma cells (163-165).

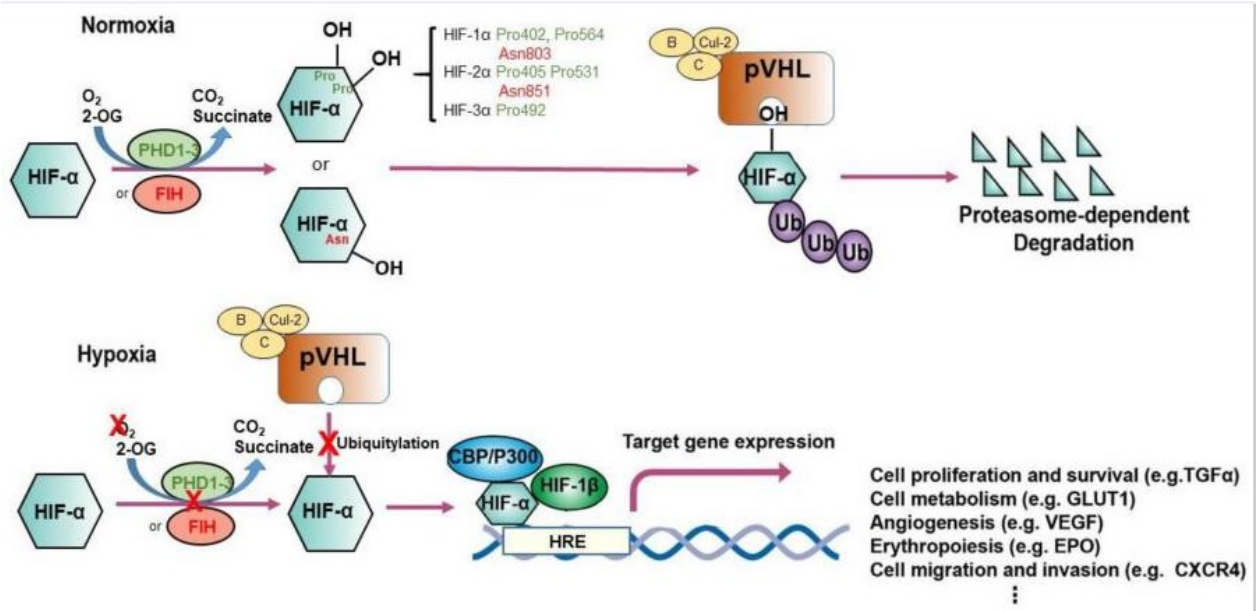

Figure 7 Hypoxia and Oxygen signalling (Yang et.al, Hypoxia and Oxygen-Sensing Signaling in Gene Regulation and Cancer Progression Int J Mol Sci. 2020 Nov; 21(21): 8162, fig. 1)

HIF can hydroxylated under normoxic state from PHD. The hydroxy group is necessary for binding to the pVH, an ubiquitin. HIF can be degraded proteasomal. Under hypoxic state, PHD cannot hydroxylate, so HIF accumulates and activates HRE in the promotor regions of the DNA. Another pathway for hydroxylation is the FIH.

Under normal oxygen conditions, blocking HIF-1 has been found to increase the susceptibility of fibrosarcoma, gastric cancer, and breast carcinoma cells to standard chemotherapy drugs (154,156,166-168).

The results of some studies suggest that HIF-1 may mediate drug resistance under normoxic conditions in certain types of human cancers. In general, HIF-1 appears to promote drug resistance in cancer cells, but there are also conflicting reports that suggest overexpression of HIF-1 can enhance tumor cell susceptibility to chemotherapy. For example, a recent study by Evens et al. found that HIF-1 expression correlated with better progression-free survival and overall survival in patients with diffuse large B-cell lymphoma treated with standard anthracycline-based chemotherapy and rituximab (169).

1.6 Aim of the Thesis

Aim of the thesis is to gain a more comprehensive understanding of two fusion-translocated sarcoma types, namely Ewing sarcoma and *CIC::DUX4* sarcoma as both sarcoma types, although similar in histological and molecular features, significantly differ in outcome and therapeutic response. A variety of molecular mechanisms regarding drug resistance is discussed focusing mainly on lipid metabolism and its role in resistance to anticancer therapy. In order to elucidate molecular mechanisms of drug resistance and malignancy, lipid profiles of the respective tumor entities are generated by mass spectrometry using 2D cell culture. Furthermore, impact of hypoxic conditions on the same tumor cells is studied in an analogous manner. For the experiments, cell lines MUG CIDUS, a patient-derived *CIC::DUX4* sarcoma continuous cell line and MHH-ES-1, an Ewing sarcoma cell line obtained from the American Type Culture Collection (ATCC) are used, serving as model systems.

2 Material and Methods

2.1 Declaration

The study was approved by the ethics committee of the Medical University of Graz (vote 31–457 ex 18/19).

2.2 Cell culture

For all experiments the patient-derived *CIC::DUX4* sarcoma cell line MUG CIDUS was used. The commercially available Ewing sarcoma cell line MHH-ES-1 was obtained from the American Type Culture Collection (ATCC, USA). The origin of MHH-ES-1 is gained from ascites of a 12-year-old boy with Ewing's sarcoma (type 2) of the left pelvis (with peritoneal metastasis), the cells carry the characteristic *EWS::FLI1* fusion gene (170). Unless otherwise stated in the individual experiments, cells were cultivated in RPMI 1640 medium (Gibco, Carlsbad, CA) supplemented with 10% foetal bovine serum (FBS, Biowest, France), L-glutamine (Gibco) and 1% penicillin/streptomycin (Gibco, Darmstadt, Germany). Cells were in general kept in a 5% CO_2 atmosphere at 37°C. For **hypoxic conditions**, cells were maintained in a hypoxic bench (Xvivo System, BioSperix, USA) at 1.6% O_2, ambient pressure of 760 mmHg and 12 mmHg O_2 partial pressure according to idealised conditions reported in literature for soft tissue sarcoma (171). Confluency was observed using the Eclipse Ti2 inverted microscope (Nikon, Tokyo, Japan), 10 × magnification, and pictures take with the numerical aperture 0.30 with a DS-Fi2 camera (Nikon, Tokyo, Japan). Pictures were analyzed with the NIS-Elements BR 5.02.00 software (Nikon, Tokyo, Japan). For cell counting cells were stained with 0.4% Trypan Blue solution (Bio-Rad, California, USA) and cell number subsequently determined using the Cellometer Auto T4 (PEQLAB®, VWR International, Inc., Erlangen, Germany). Cell lines were regularly checked for mycoplasma and authenticated with STR analysis.

2.3 Mass-spectrometry

Chemicals

Acetonitrile, ammonium formate (LC/MS grade), isopropanol, methanol and tert-methyl-butyl, ether (MTBE) (all Chromasolv grade), were obtained from Sigma-Aldrich (St. Louis, MO, USA), while chloroform and formic acid were purchased from Merck (Darmstadt, Germany). An in-house MilliQ Gradient A10 system (Millipore, Billerica, MA, USA) supplied deionized water.

Lipid extraction

Used samples: MHH-ES-1, Passage: pZB+14, Mycoplasm tested, STR profile: MHH-ES-1
MUG CIDUS, Passage: 27, Mycoplasm tested, STR Profile: MUG CIDUS

Each sample contains the lysate of $1*10^6$ cells (see in appendix **Table 1**).

A modified version of the lipid extraction protocol originally published by (172) was used in this study. Sarcoma samples (1 mL of methanol) were mixed with 0.5 mL of methanol and 2.5 mL of MTBE in 12 mL glass tubes with Teflon-lined caps. The samples were homogenized for 30 seconds using an Ultra-Turrax tissue homogenizer (IKA Works Inc., Wilmington, N.C., USA). After adding 2.5 mL of MTBE and shaking for 10 seconds, the mixture was incubated in an ice-cooled ultrasound bath for 10 minutes. After the addition of 1.25 mL of deionized water and shaking the mixture overhead for 10 minutes, it was centrifuged at room temperature for 10 minutes at 1350 g. Subsequently, the upper phase was carefully transferred into a new glass tube. The lower phase was subjected to a second extraction using 2 mL of MTBE/methanol/deionized water (10:3:2.5, v/v/v) from the upper phase. Subsequently, the upper phase obtained from this extraction was pooled with the upper phase collected in the initial extraction. The combined upper phase was then dried using a vacuum centrifuge (Thermo Fisher Scientific, Waltham, MA, USA). The resulting residue was dissolved in 1000 µL of chloroform/methanol (1:1, v/v) and stored at -80 °C.

For quantification, a mixture of internal standards was added to 30 µL of the extract. Subsequently, the solvent was evaporated using a gentle stream of nitrogen, and the resulting residue was reconstituted in 90 µL of injection solvent composed of isopropanol/chloroform/methanol (90:5:5, v/v/v).

LC method - lipids

The chromatographic separation was carried out following the method described in (173). In brief, a Waters BEH C8 column (100 × 1 mm, 1.7 µm) was used and thermostatted to 50 °C in a Dionex Ultimate 3000 RS UHPLC system (Waters, Milford, MA, USA). Mobile phase A consisted of deionized water containing 1 vol% of 1 M aqueous ammonium formate (final concentration 10 mmol/L) and 0.1 vol% of formic acid as additives, while mobile phase B was a mixture of acetonitrile/isopropanol 5:2 (v/v) with the same additives. The gradient elution started at 50% mobile phase B and increased to 100% B over 15 minutes, with 100% B being held for 10 minutes. The column was then re-equilibrated with 50% B for 8 minutes before the next injection. The flow rate was maintained at 150 L/min, the samples were kept at a temperature of 8 °C, and the injection volume was set at 2 µL.

MS method - lipids

The Orbitrap Velos Pro hybrid mass spectrometer (Thermo Fisher Scientific Inc., Waltham, MA, USA) was operated in Data Dependent Acquisition (DDA) mode for every sample, using positive polarity mode and a HESI II ion source. The ion source parameters were set as follows: Source Voltage: 4.5 kV, Source Temperature: 275 ◦C, Sheath Gas: 25 arbitrary units, Aux Gas: 9 arbitrary units, Sweep Gas: 0 arbitrary units, Capillary Temperature: 300 ◦C. The target value for automatic gain control was established at 106 ions, which were allowed to enter the mass analyzer with a maximum ion accumulation time of 500 ms. In positive ion mode, full scan profile spectra were obtained using the Orbitrap mass analyzer, covering the m/z range from 320 to 1050, with a resolution setting of 100,000 at m/z 400. In the MS/MS experiments, the ten most abundant ions (Top 10) from the full scan spectrum for further analysis was selected. These chosen ions were then sequentially fragmented in the ion trap, utilizing helium as the collision gas (CID), and the following specific parameters were applied: Normalized Collision Energy: 50, Isolation Width: 1.5, Activation Q: 0.2, Activation Time: 10, and centroid product spectra were collected at a normal scan rate of 33 kDa/s. The LC/MS data were processed utilizing the Lipid Data Analyzer (LDA) software (174,175), which utilizes a three-dimensional algorithm. This algorithm takes into account the dimensions of m/z, retention time, and intensity to accurately integrate peaks, while also considering the isotopic distribution. MS/MS spectra were also used to confirm lipid structures based on characteristic head group and fatty acyl

fragments.

2.4 Statistical Analysis

Statistical significance was calculated by the Mann-Whitney-U test without the assumption of a normal distribution of the dependent variable in the two groups. Evaluation was performed using the SPSS Statistics 26 software (IBM, USA). All data were reported as mean ± standard deviation, n denoting the number of independent experiments. $P<0.05$ were considered as significant (* 0.01 to 0.05, **0.001 to 0.01, *** < 0.001)

3 Results

3.1 Patient History

The cell line MUG CIDUS had been isolated from tumor tissue available as surgical specimen of the following patient. In October 2019, a 60-year-old male patient was referred to the Department of Orthopaedics and Trauma at the Medical University of Graz due to severe pain in the right groin. Magnetic resonance imaging (MRI) of the pelvis revealed an 11 cm tumor in the right iliac muscle. A biopsy performed in November 2019 confirmed a high-grade undifferentiated round cell sarcoma involving the *CIC::DUX4* fusion gene. Further chest CT showed multiple metastases in both lungs. In the following month, due to drug-resistant pain and the patient's request, surgery was performed to remove the primary tumor. The histopathological evaluation confirmed the biopsy diagnosis, but revealed a marginal (R1) resection. The sample, from which the cell line was established, was taken on 09.12.2019. In January 2020, chest CT showed progression of the lung metastases, and the patient started palliative chemotherapy with vincristine, adriamycin, ifosfamide, alternating with vincristine, actinomycin D, and ifosfamide at the Division of Clinical Oncology. In April 2020, chest CT showed partial remission of the lung metastases, and the patient was pain-free. The chemotherapy continued for a total of 11 cycles until August 2020, when it was stopped at the patient's request. Pelvic MRI showed no signs of tumor progression, and chest CT revealed ongoing partial remission with only residual lung metastases. However, in October 2020, the patient experienced recurrence of pain in the right groin, and imaging confirmed local recurrence of the primary tumor and progression of lung metastases. Palliative radiation therapy of the right iliopsoas muscle area was performed in the following month. Additionally, chemotherapy with vincristine, adriamycin, ifosfamide, alternating with vincristine, actinomycin D, and ifosfamide was reinitiated, resulting in partial remission after 4 cycles in March 2021. At this stage, the chemotherapy was discontinued due to cardiac toxicity. Subsequently, the patient underwent maintenance treatment with cyclophosphamide and celecoxib. However, in April 2021, this treatment was halted due to disease progression in the lung metastases, and was switched to irinotecan and temodal. After three cycles in June 2021, the chemotherapy was changed again to topotecan and cyclophosphamide as the primary tumor continued to progress. Three months later, a pelvis MRI and chest CT revealed progressive disease (Figure 8 A-F). As a result, chemotherapy with gemcitabine and docetaxel was initiated. In November 2021, the patient

presented with symptoms such as headache, confusion, and coordination disturbances. A brain MRI revealed a 5 cm solitary brain metastasis in the left posterior lobe (Figure 8 G-H).

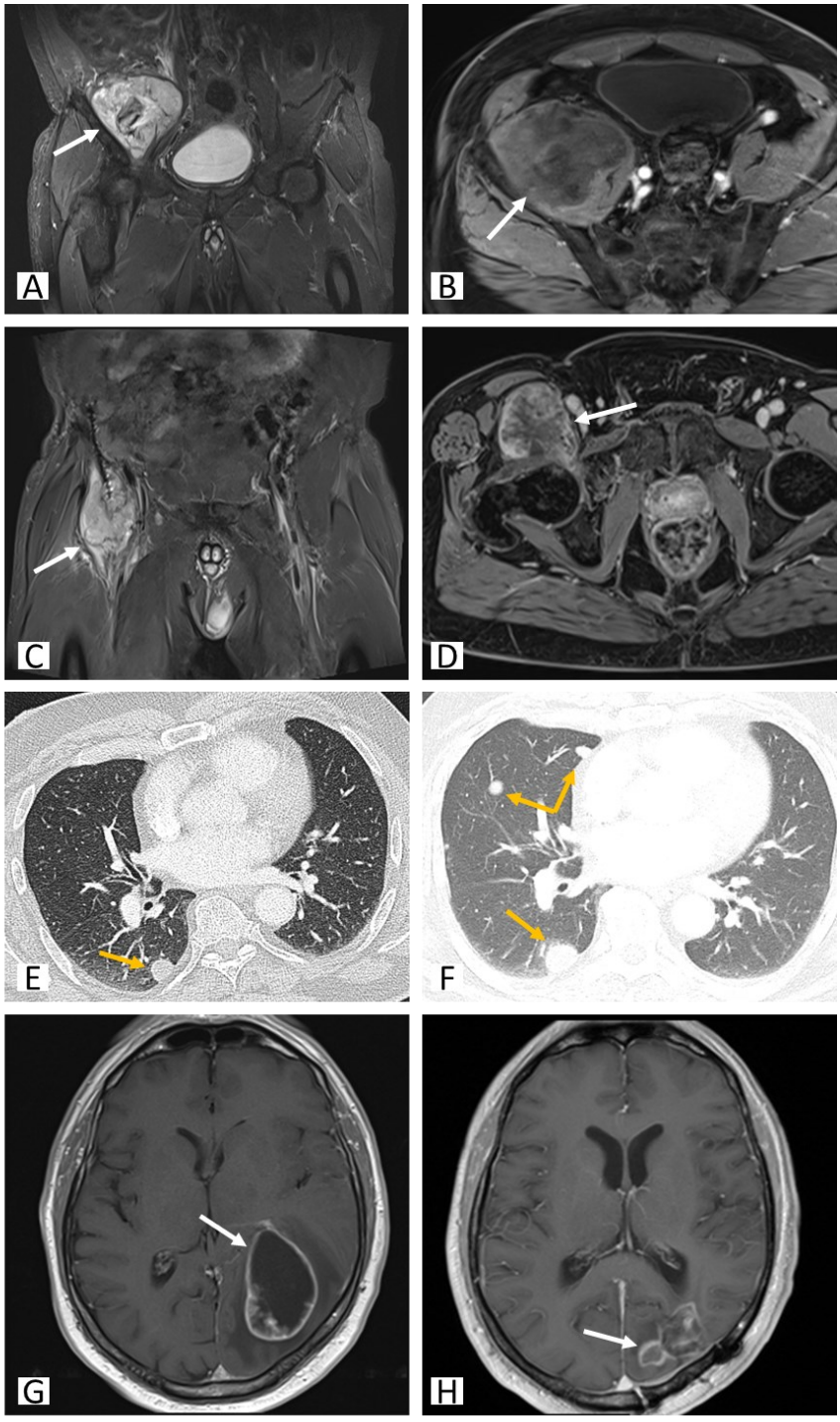

Figure 8 Patient examinations
Initial MRI examination of the pelvis (November 2019) in T2-weighted FS coronal image (A) and axial T1-weighted image (B) after intravenous application of Gadolinium (contrast agent), shows a heterogenous soft-tissue expansive intramuscular lesion in the right iliac muscle with a maximal diameter of 11cm and a high signal in fluid-sensitive sequence, corresponding to myxoid tissue (A). Postcontrast, central necrotic parts are demarcated

with peripheral contrast-enhancement (B). Eleven months after marginal palliative resection, the patient developed a 7 cm local recurrence in the right thigh along the postoperative scar with infiltration of the femoral vessels and nerves, so as infiltration of quadriceps muscle, seen on coronal T2-weighted image (C). Heterogeneous contrast-enhancement of the lesion with infiltration of the joint capsule (D). Initial high resolution CT-staging examination (November 2019) in the lung window showed the presence of bilateral lung metastasis (E), progressive on follow-up examination in 6-weeks-interval (F). At MRI examination of the brain two years after initial diagnosis, the patient developed a 5 cm cerebral metastasis in the left posterior lobe with peripheral contrast enhancement (G). The lesion was resected, following with nodular relapse at the resection margin 6 months after the operative treatment (H).

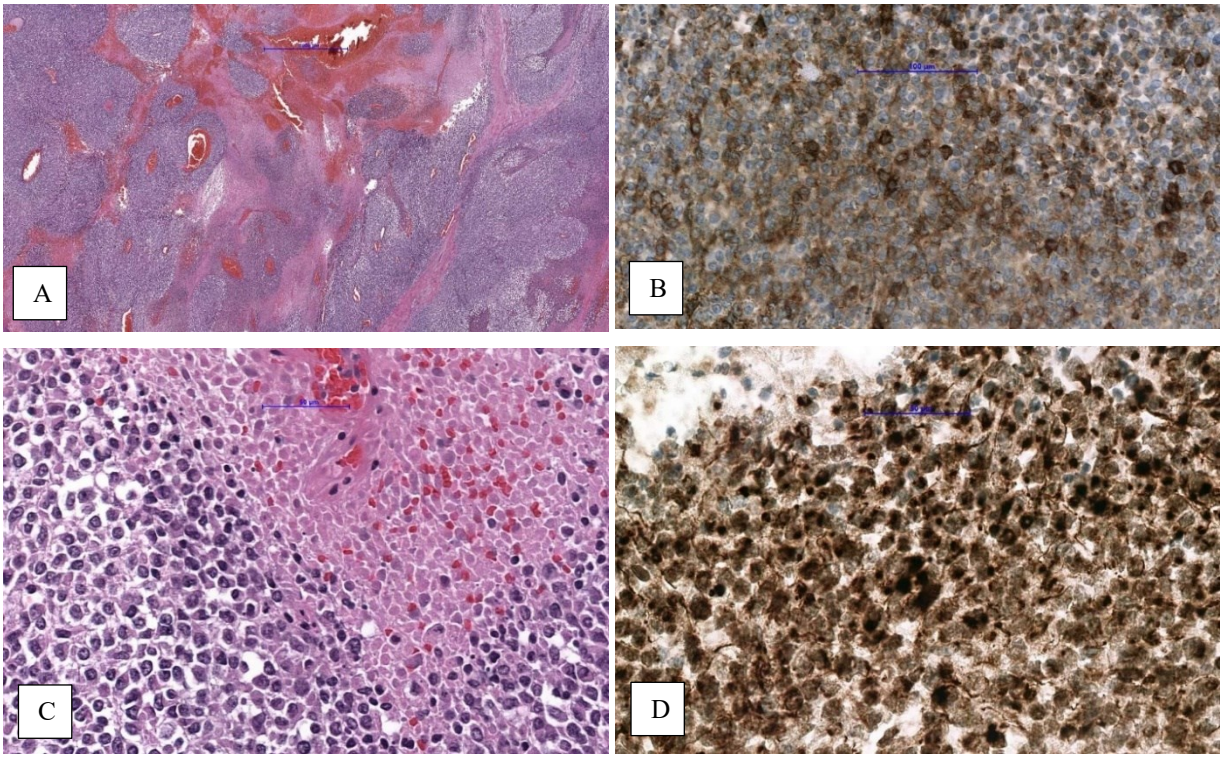

Figure 9, Histologic images of the patient

Small and round cells in a solid, nodular growth pattern and perivascular cell preservation, multiple foci of necrosis could be found (A, C). A strong membranous CD99 (B) and nuclear WT1 (D) expression could be observed in the tumor. The tumor is composed of tumor cells with round nuclei and "plasmacytoid" morphology. The nuclei are excentrically located and surrounded by eosinophilic cytoplasm. The individual nuclei are enlarged. Necrotic cells are seen (C). Scale bars depicted are 1000 µm (A), 100 µm (B) and 50 µm (C, D).

The brain metastasis was surgically removed, followed by local postoperative radiation therapy. Subsequently, the patient's neurological symptoms improved. The histopathological report confirmed that the brain metastasis was consistent with the previously diagnosed *CIC::DUX4* fusion gene-associated sarcoma. In February 2022, the patient received chemotherapy with caelyx (doxorubicin) and ifosfamide. However, after three months, the patient experienced recurrence with two brain metastases, which were treated with stereotactic radiation therapy. Additionally, the patient reported increasing pain in the right groin, which was managed with a high-dose morphine-based pain therapy. Meanwhile, next-generation sequencing (NGS) testing

with FoundationOne Liquid CDx was conducted, revealing an ATM + RAD51C mutation and a high tumor mutational burden (TMB-H), a marker who is not fully understood to predict response to immune checkpoint blockade (176) . Given that ATM-mutant cells are known to have defective DNA repair and are predicted to be sensitive to platinum drugs (177) that induce double-strand DNA breaks. Previous existing clinical data supporting the use of TMB as a predictive biomarker for immune checkpoint inhibitors (178), a combination treatment with carboplatin, etoposide, and pembrolizumab was begun in June 2022 when a progress in disease was identified in the pelvis MRI and chest CT. Unfortunately, this treatment had to be discontinued after 2 cycles due to disease progression. By this time, the patient required a wheelchair due to extensive progression of the primary tumor. In September 2022, the patient received one cycle of trabectedin and underwent whole brain irradiation for progressive cerebral metastases. However, the patient passed away in the same month due to multi-organ failure.

3.2 Study Design

All experiments were performed using cell culture as an *in vitro* model system. As *CIC::DUX4* sarcoma are ultra rare, the cell line used, MUG CIDUS, resulted from in-house generation, whereas the Ewing Sarcoma cell line MHH-ES-1 was chosen as it is commercially available, frequently used and well established in literature. Both cell lines still harbour their characteristic tumor-driving gene fusion, *CIC::DUX4* and *EWS::FLI1*. Morphological differences between the cell lines are elucidated in Figure 9.

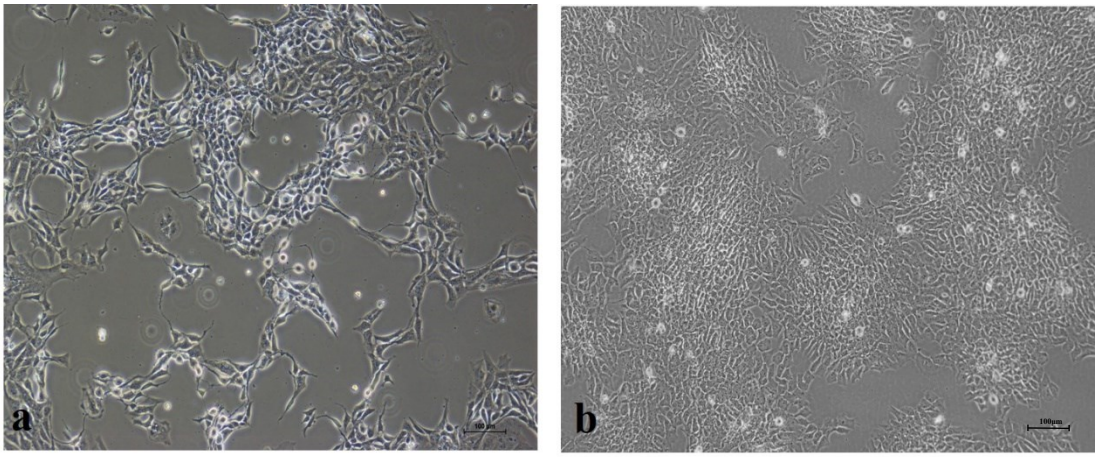

Figure 10 Cell morphology
CIC::DUX4 sarcoma cell line MUG CIDUS (a) and Ewing Sarcoma cell line MHH-ES-1 (b). Scale bars depicted are 100 µm.

For lipid profiling LC/MS was used to quantify a variety of lipid classes including triglycerides (TG). The phospholipids phosphatitylcholine (PC), phosphatitylethanolamine (PE) phosphatylserine (PS), sphingomyelin (SM), ceramides (CER) and cholesterol (CHOL) in lipid extracts of these two cell lines. Lipid classes that were analysed are depicted in Figure 10 as well as the specific distribution of individual species per class detected. In addition to the two cell lines, two growth conditions per cell line were also analysed. Once under atmospheric conditions and once under tissue-typical partial pressure of a soft tissue sarcoma at 1.6% (hypoxia).

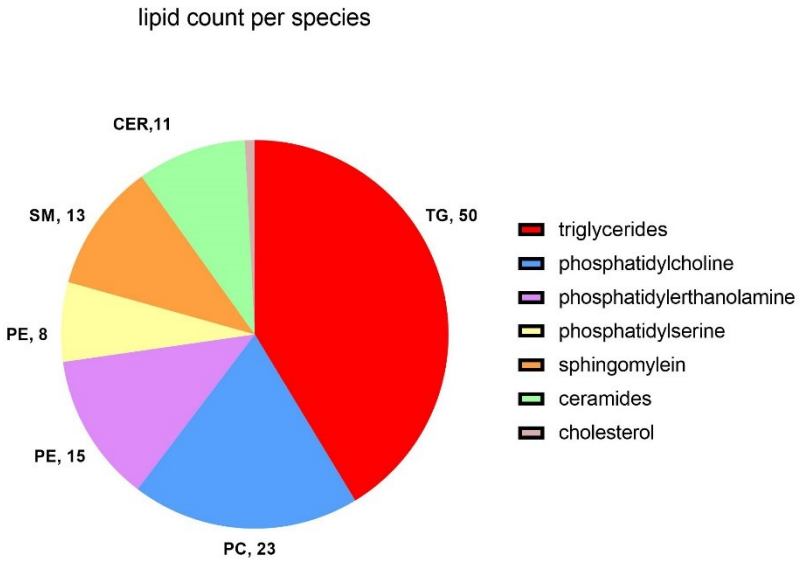

Figure 11 Distribution of lipid classes
Lipid classes and respective count of representative molecular species per class detected in the study. Analysis was performed analogously for both cell lines, detecting triglycerides (TG), phospholipids (PL), ceramides (CER) and cholesterol (CHOL).

3.3 Influence of hypoxia on the lipid signature of sarcoma cells

In order to achieve a general overview of the lipid composition of the cell line MUG CIDUS and MHH-ES-1, we performed LC-MS. To enable better comparison between those two, the same cell number, namely 1×10^6 cell were used for lipid extraction and subsequent experiment. To mimic the physiological environment of the tumor cells *in vitro*, lipidomes were compared not only under normoxic, but also hypoxic conditions. Interestingly, hypoxia altered the lipid metabolism of MUG CIDUS by increasing all TG and CER species, but only a few phospholipid species with most of them, showing decreased values compared to normoxia. On the other hand,

MHH-ES-1 only showed a prominent increase for all CER species, whereas for all other lipids no overall trend could be observed. In contrast to MUG CIDUS, increase in TG was only evident for shorter fatty acid residues, whereas the majority of long-chain TG decreased under hypoxia. CHOL levels did not change under hypoxic conditions, neither in MUG CIDUS nor in MHH-ES-1.

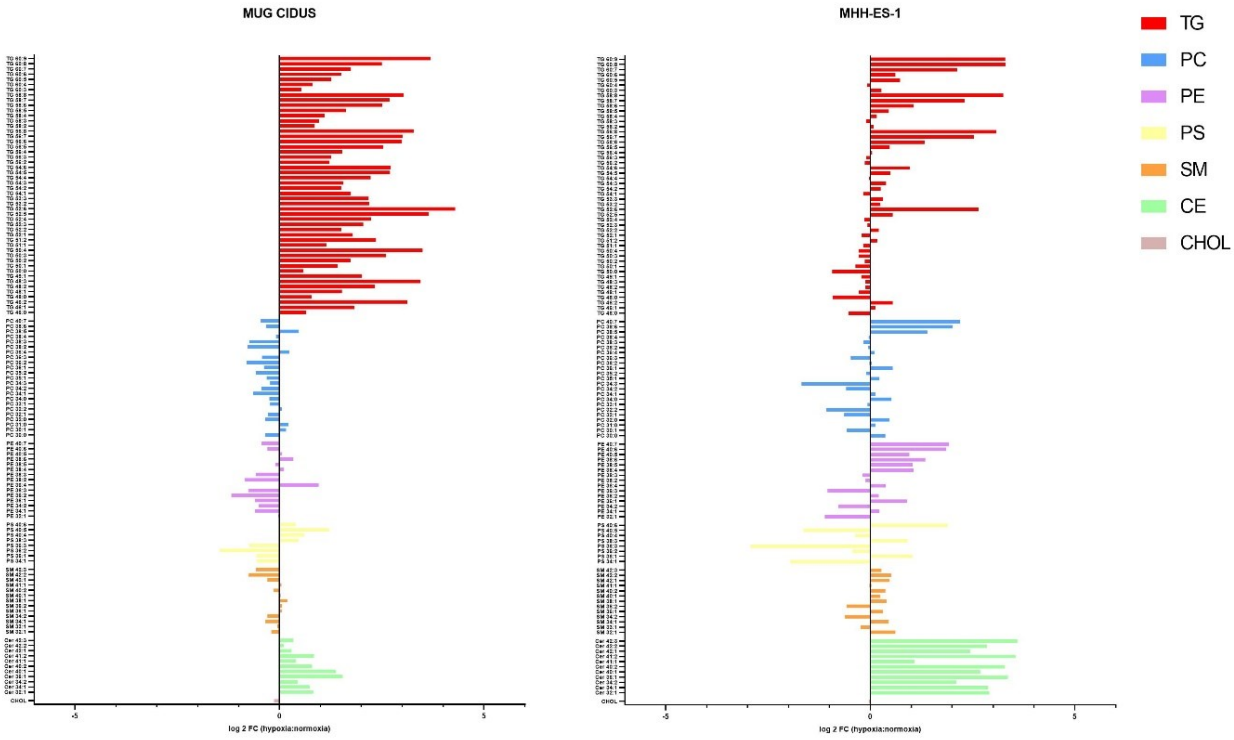

Figure 12 Impact of hypoxia on the lipidome
MUG CIDUS (left) and MHH-ES-1 (right). Data are portrayed as log2FC and represent mean of five replicates.

3.4 Long chain triglycerides accumulate in MUG CIDUS under hypoxic conditions

To specify the analysis, we next looked at the lipid species separately and compared these directly between the two cell lines. Interestingly, MUG CIDUS cells only portrayed significantly higher TG levels per 1×10^6 cells than MHH-ES-1 under hypoxic conditions. Also, hypoxia affected only long-chain (C>54) and saturated MUG CIDUS TG, yielding in increased levels compared to MHH-ES-1, whereas under both normoxic and hypoxic conditions MHH-ES-1 dominantly exhibited higher levels for shorter fatty acid chain lengths (Figure 13).

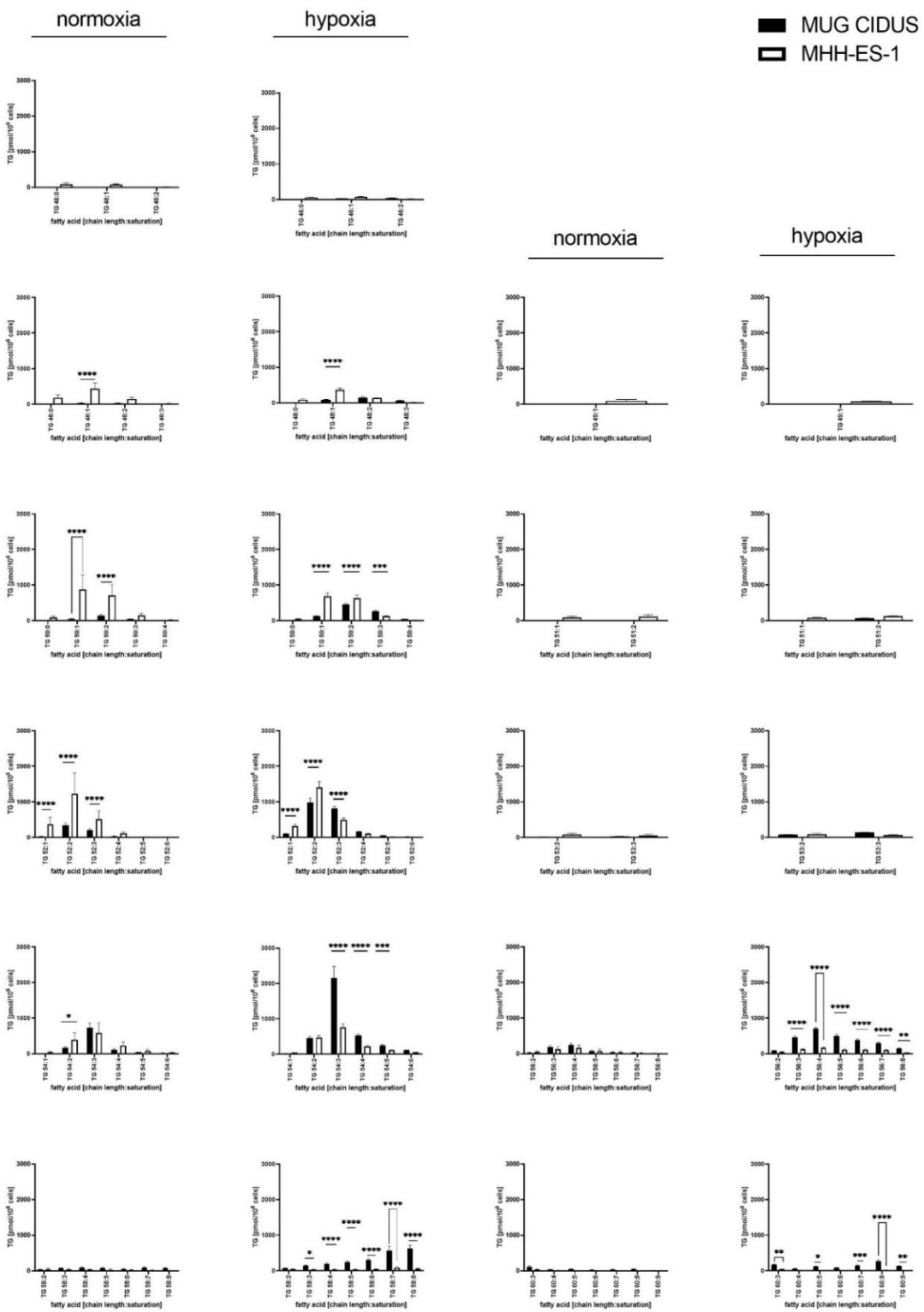

Figure 13 Triglyceride profile

Triglyceride levels for each chain length with increasing saturation degree compared between MUG CIDUS and MHH-ES-1. Results represent mean ± standard deviation.

3.5 Phospholipids

Next, we evaluated the phospholipid (PL) and the respective fatty-acid composition of the cell lines. The same analytical approach used for the previous lipid classes, was applied for analysis of the phospholipid contents and comparison between the cell lines. Results for individual species of PC, PE, PS and SM species are presented in Figure 14.

PC species were overall more abundant in MUG CIDUS, especially under normoxic conditions. However, under hypoxic conditions several PC levels decreased for MUG CIDUS but we found only one PC species (PC 36:1) to be significantly increased in MHH-ES-1 compared to MUG CIDUS.

Again, almost all PE species were more abundant in MUG CIDUS under normoxic conditions, which changed in a hypoxic atmosphere. In both PE profiles, four discriminating species (34:1, 34:2, 36:2, 38:5) were identified, with elevated levels characteristic to MUG CIDUS. However, PE levels in total did decrease under hypoxia for some of the mentioned species, but the overall trend persisted. Interestingly, although the trend remained the same for these respective PL levels, there were additional species elevated under hypoxic conditions, but for MHH-ES-1. In context, SM 36:1, SM 38:4 and SM 40:6 were the only ones affected by hypoxia in MHH-ES-1, increasing significantly, whereas under normoxic conditions for these species no differences between the cell lines were detected (Figure 14, b).

For PS, only three species, PS 34:1, 36:1 and 36:2, were observed to significantly differ between the cell lines under hypoxic conditions. PS 36:1 and PS 40:6 are the only species out of the mentioned four, that are more abundant in MHH-ES-1 compared to MUG CIDUS. Furthermore they are also the only species that increase under hypoxic conditions in MHH-ES-1 cells. Although MUG CIDUS depicts the same trend under both conditions for PS 34:1, 36:1 and 36:2, the total amount of these respective molecular species decreases in all three cases. Longer FA chain species, except PS 40:6, do not seem to be affected by hypoxia and show similar patterns for both tumor cell lines (Figure 14, c).

Similar to PS, MUG CIDUS reduces the accumulation of the as significant marked SM species (SM 34:1, 36:1, 42:2) under hypoxia. In contrast, MHH-ES-1 enhances its amount for the same species and additionally for SM 42:1. Under normoxic conditions, MUG CIDUS forms a significant higher amount of SM in total (Figure 14, d).

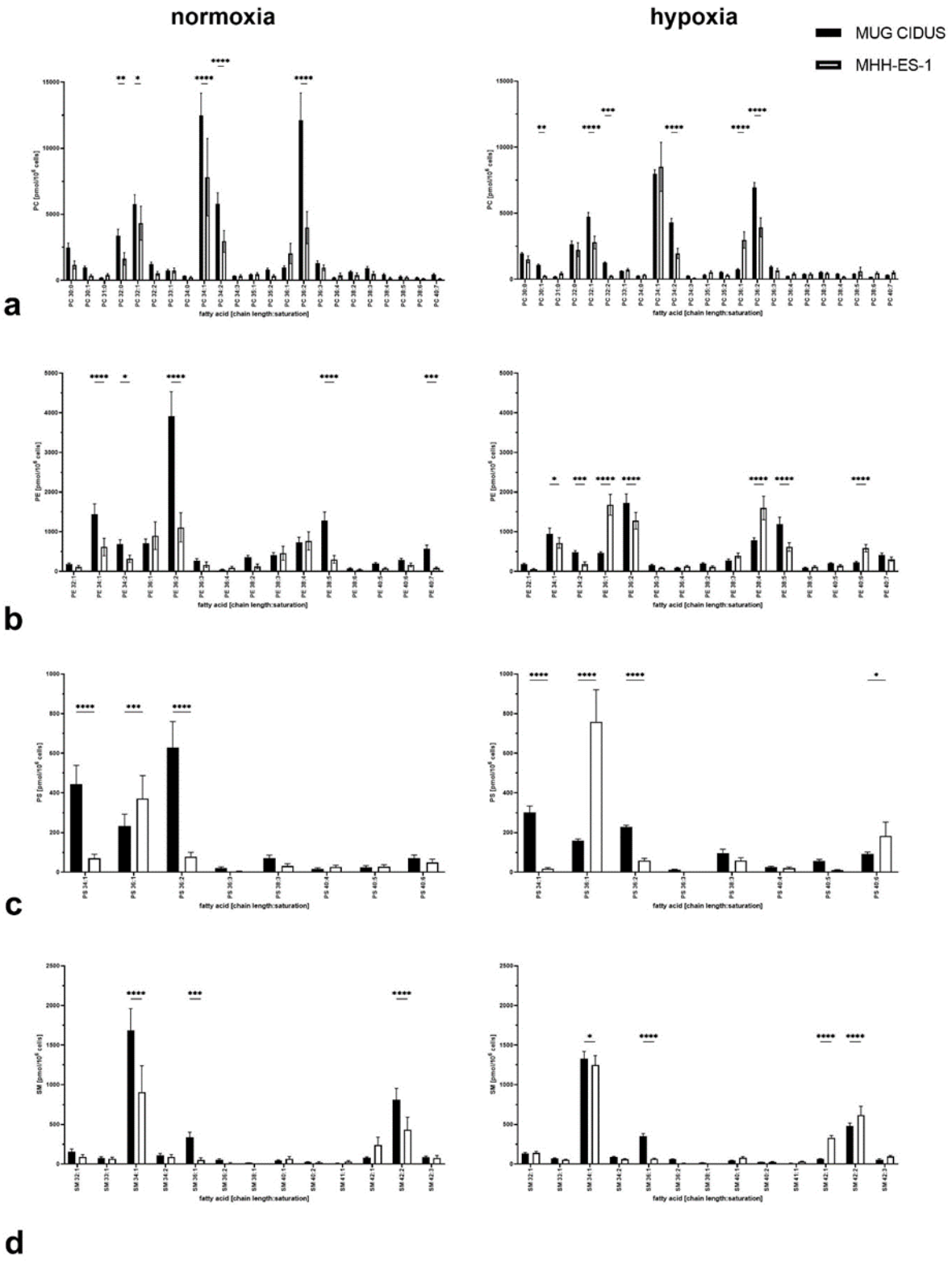

Figure 14 Phospholipid profile
Amount of phospholipids over the chain length. Results represent the mean and ± standard deviation.

3.6 Ceramides and cholesterol levels minimally differ in CDS and ES cell lines

CER levels only showed significant differences for CER species 34:1 and 42:2 under both conditions. However, under normoxic conditions MUG CIDUS exhibits generally elevated levels compared to MHH-ES-1, whereas under hypoxic conditions the opposite is true. In addition, hypoxic conditions especially increase levels of CER 42:1 for MHH-ES-1 significantly (Figure 15a). For CHOL, no significant differences between the cell lines could be observed neither under hypoxia nor under normoxia (p = 0.15 and 0.54, Figure 15b).

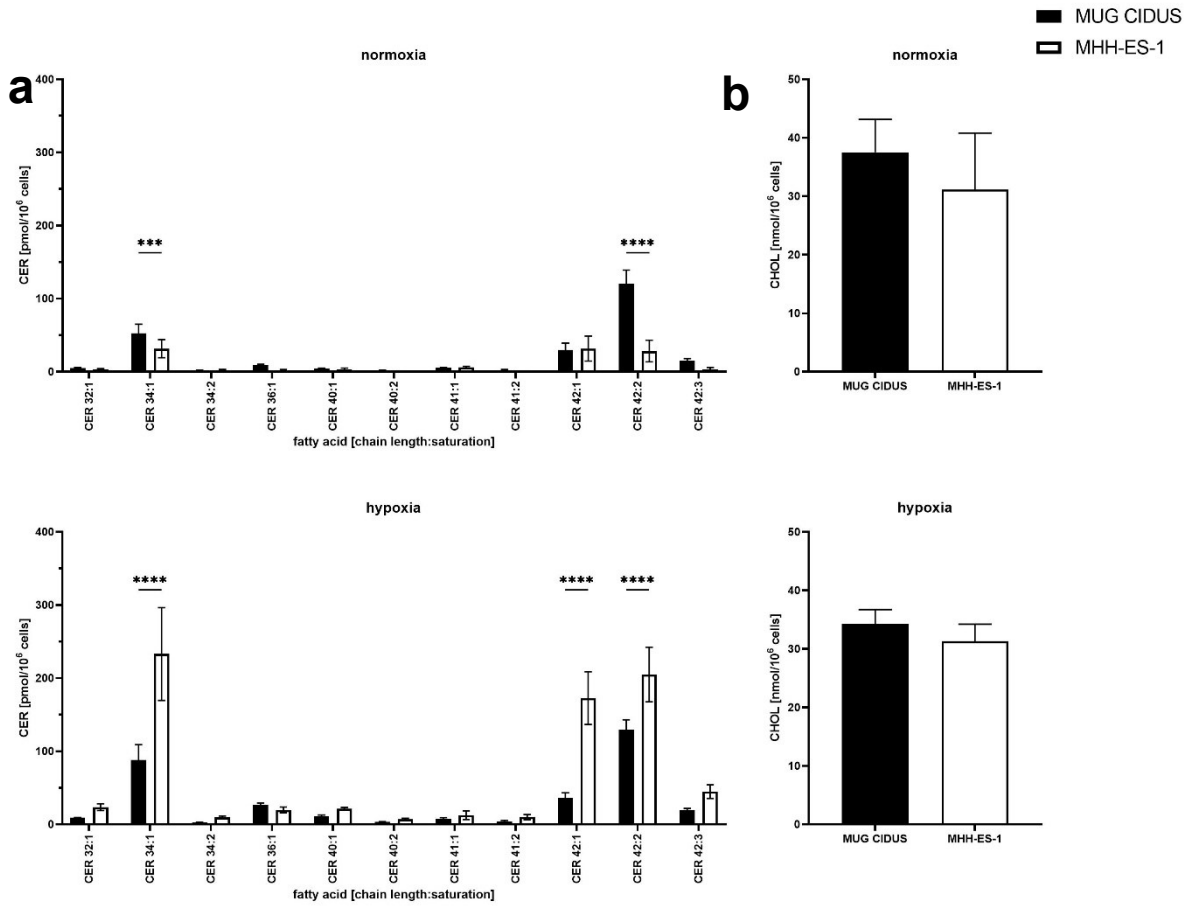

Figure 15 Ceramides and cholesterol
CER and CHOL per chain length and saturation degree. Results represent the mean of five replicates ± standard deviation.

4 Discussion

In the current WHO Soft Tissue and Bone Tumor (2020), a new chapter of undifferentiated small round cell sarcomas of bone and soft tissue has been introduced. Desoite Ewing Sarcoma, three additional molecularly defined tumor groups have been included (a) Round cell sarcoma with EWSR1 – not ETS fusions, (b) CIC – rearranged Sarcoma and (c) Sarcoma with BCOR alterations (44) .

They consistently appear to be less chemo-sensitive than the classic Ewing sarcoma, but are still managed by the same treatment regimen. The high frequency of relapse in localised disease, poor treatment response and fatal outcome further elucidates the distinct clinical outcome of CIC-rearranged sarcoma in comparison to Ewing sarcoma (179).

Several different chemotherapeutic agents have already been tested in preclinical studies (180-182). The standard treatment protocol for CDS is doxorubicin together with vincristine or cyclophosphamide alternating with ifosfamide and etoposide (179) as the North American regime or the Euro-Ewing trial with vincristine, doxorubicin, ifosfamide and etoposide (183). According to Oyama et al., doxorubicin has demonstrated notable effectiveness in a well-established in vitro model of CDS (184). However, it is important to note that, overall, doxorubicin yields unsatisfactory outcomes in patients. This study, therefore, tried to find an explanation why *CIC::DUX4* sarcoma, in particular, is more resistant to chemotherapeutic agents in comparison to Ewing sarcoma, another member of the small, blue round cell group of sarcomas. In Ewing sarcoma, the use of chemotherapy improved the 5 year overall survival of patients with localized disease from 10 to 70% (185). One way to build up a chemoresistance is an altered lipid metabolism (186). To investigate this, lipid profiling by mass spectrometry of cell lines, MUG CIDUS (CDS) and MHH-ES-1 (ES) representative of the two tumor entities was carried out. Furthermore, to assess the impact of the hypoxic environment on lipid metabolism, all cell lines were also analysed under hypoxic conditions. Recent literature suggests, that a lack of oxygen forces the tumor to adapt and use another metabolic pathways and the origin tumor microenvironment was mimicked too (187).

The lipidomic study revealed an accumulation of all TG in hypoxic MUG CIDUS cells, whereas in MHH-ES-1 both increases and decreases in TG levels could be observed depending on the condition. This indicates the accumulation of excess FAs in cellular TG stores. These observations raise the possibility of lipid droplet (LD) formation, as the core of those mainly

consists of TG and sterol esters. Yosef et al. demonstrated the aberrant accumulation of LDs in *KRAS* and *BRAF* mutated colon cancer associating the formation of the respective to erlotinib resistance (188). Also, in breast cancer, myeloid leukaemia and lung cancer, drug sequestration into LDs (189-191) was reported to promote chemoresistance by reducing cytoplasmic drug concentrations.

Compounds exhibiting pronounced hydrophobicity might become trapped within accumulating lipid droplets (LDs), compromising their anti-cancer efficacy and explaining their lack of impact in vivo. However, to truly establish a correlation with drug resistance, it is imperative to provide concrete evidence of LD accumulation in MUG CIDUS rather than solely observing an increase in TG levels.

Next, we evaluated phospholipid profiles. Phospholipids are the main component of the lipid bilayer directly, contributing to the cellular structure. Hypoxia induced severe decreases in all PL classes of MUG CIDUS, especially PE, PC and SM, which was not the case in MHH-ES-1. An increase in CER under hypoxia could be detected in both cell lines, but in MHH-ES-1 the increase was significantly higher (L2FC ~ 3). Of note, hypoxia induced in MUG CIDUS an increase in CER, but a decrease in SM, whereas in MHH-ES-1 induced a decrease only in 3 out of 10 detected SM species. CER can be generated by SMAs (sphingomyelinase), which cleave PC or PE from SM. Under cellular stress, e.g.,chemotherapy, especially therapy resistant tumour cells try escaping apoptosis by decreasing the activity of this enzyme, as the release of CER usually has anti-cancer properties and leads to cell death by apoptosis (192). Although both cell lines were able to produce CER, MUG CIDUS generated significantly less CER under hypoxia than MHH-ES-1, indicating that MUG CIDUS is less sensitive to cellular stress than MHH-ES-1. As described in Chapter 1.4.1, this is a characteristic of MDR cells. To further validate this hypothesis, levels of SMAs activity should be analyzed under hypoxia..

Last, the influence of CHOL on resistance could be refuted in comparison to MHH-ES-1. No significant difference could be detected between the two cell lines MUG CIDUS and MHH-ES-1, neither under hypoxia ($p=0.151$) nor under normoxia ($p=0.548$), which resulted in the conclusion that cholesterol metabolism did not play a significant role in differentiating between ES and CDS in regards to their drug sensitivity.

Normalization and reliable comparison between cell lines is complex, so it is important to

mention, that the study has several limitations. First, normalization of the quantified lipids was based on cell number, however no protein levels were additionally determined for a more comprehensive evaluation. Although the used cell lines are similar, to verify and optimize comparability, it would still be necessary to assess aspects like a variety of levels on the molecular level (DNA, RNA, protein), cell size and doubling time as the growth behaviour is associated with metabolic activity as well. Furthermore, only one cell line of the *CIC::DUX4* sarcoma and one Ewing sarcoma cell line were used, reflecting only two patients, respectively. The cell lines do carry their molecular characteristic and tumour driving oncogene. The Ewing sarcoma cell line MHH-ES-1 has the most frequent (85%) fusion but other forms of oncogenic fusions exist, which could have an impact on lipid metabolism, meaning that a subtype of the same histologic tumour entity could show different results (193). This is further limited by the rarity of these subtypes, making it difficult to expand the cohort of the study.

The study indicates an association of lipid metabolism involved in drug resistant behaviour of *CIC::DUX4* sarcoma, but more experiments are needed to underpin this hypothesis. Next, doxorubicin sensitivity should be evaluated under normoxic and hypoxic conditions for both cell lines. Transcriptomic profiling of the same cell lines could also give further information on gene expression alterations associated with lipid metabolism under hypoxia. Also, the differences in lipid signatures between normal healthy cells and tumor cells should be investigated to gain a better understanding of the importance of lipid metabolism in *CIC::DUX4* sarcoma. Altogether, the study portrays a fundament for future experiments and gives insight into the characteristics of the ultra-rare *CIC::DUX4* sarcoma, for which novel therapeutic options are desperately needed.

Literature

(1) Yuning Tang. Investigation of Intratumoral Heterogeneity in Sarcoma Progression and Metastasis: From Tumor Propagating Cell Dynamics to Clonal EvolutionUniversity of Toronto, Canada; 2019.

(2) Sbaraglia M, Bellan E, Dei Tos AP. The 2020 WHO Classification of Soft Tissue Tumours: news and perspectives. Pathologica 2021 Apr;113(2):70-84.

(3) Zhao X, Yue C. Gastrointestinal stromal tumor. J Gastrointest Oncol 2012 Sep;3(3):189-208.

(4) Anttila S, Boffetta P. Occupational cancers. : Springer; 2020.

(5) Burningham Z, Hashibe M, Spector L, Schiffman JD. The epidemiology of sarcoma. Clin Sarcoma Res 2012 Oct 4;2(1):14-14.

(6) Bray F, Ferlay J, Laversanne M, Brewster DH, Gombe Mbalawa C, Kohler B, et al. Cancer Incidence in Five Continents: Inclusion criteria, highlights from Volume X and the global status of cancer registration. Int J Cancer 2015 Nov 1;137(9):2060-2071.

(7) Brouns F, Stas M, De Wever I. Delay in diagnosis of soft tissue sarcomas. Eur J Surg Oncol 2003 Jun;29(5):440-445.

(8) Impact of Sarcoma: National Sarcoma Survey 2020. 2020; Available at: https://sarcoma.org.uk/policy-at-sarcoma-uk/impact-of-sarcoma-national-sarcoma-survey-2020/, 2023.

(9) Soomers V, Husson O, Young R, Desar I, Van der Graaf W. The sarcoma diagnostic interval: a systematic review on length, contributing factors and patient outcomes. ESMO Open 2020 Feb;5(1):e000592. doi: 10.1136/esmoopen-000592.

(10) Park JH, Kang CH, Kim CH, Chae IJ, Park JH. Highly malignant soft tissue sarcoma of the extremity with a delayed diagnosis. World J Surg Oncol 2010 Sep 23;8:84-84.

(11) Edwards M, Halton J, Ramphal R, Johnston D. Is time of the essence? Delayed diagnosis of Ewing's sarcoma. BMJ Case Rep 2015 Jan 27;2015:10.1136/bcr-208307.

(12) Arifi S, Belbaraka R, Rahhali R, Ismaili N. Treatment of Adult Soft Tissue Sarcomas: An Overview. Rare Cancers Ther 2015;3(1):69-87.

(13) Mitelman F, Johansson B, Mertens F. The impact of translocations and gene fusions on cancer causation. Nat Rev Cancer 2007 Apr;7(4):233-245.

(14) Helman LJ, Meltzer P. Mechanisms of sarcoma development. Nat Rev Cancer 2003 Sep;3(9):685-694.

(15) Osuna D, de Alava E. Molecular pathology of sarcomas. Rev Recent Clin Trials 2009 Jan;4(1):12-26.

(16) Matushansky I, Maki RG. Mechanisms of sarcomagenesis. Hematol Oncol Clin North Am 2005 Jun;19(3):427-49, v.

(17) Rodriguez R, Rubio R, Menendez P. Modeling sarcomagenesis using multipotent mesenchymal stem cells. Cell Res 2012 Jan;22(1):62-77.

(18) Lye KL, Nordin N, Vidyadaran S, Thilakavathy K. Mesenchymal stem cells: From stem cells to sarcomas. Cell Biol Int 2016 Jun;40(6):610-618.

(19) Weissferdt A, Kalhor N, Moran CA. Ewing sarcoma with extensive neural differentiation: a clinicopathologic, immunohistochemical, and molecular analysis of three cases. Am J Clin Pathol 2015 May;143(5):659-664.

(20) Folpe AL, Goldblum JR, Rubin BP, Shehata BM, Liu W, Dei Tos AP, et al. Morphologic and immunophenotypic diversity in Ewing family tumors: a study of 66 genetically confirmed cases. Am J Surg Pathol 2005 Aug;29(8):1025-1033.

(21) Sbaraglia M, Righi A, Gambarotti M, Dei Tos AP. Ewing sarcoma and Ewing-like tumors. Virchows Archiv 2020;476(1):109-119.

(22) Jimenez RE, Folpe AL, Lapham RL, Ro JY, O'Shea PA, Weiss SW, et al. Primary Ewing's sarcoma/primitive neuroectodermal tumor of the kidney: a clinicopathologic and immunohistochemical analysis of 11 cases. Am J Surg Pathol 2002 Mar;26(3):320-327.

(23) Komforti MK, Sokolovskaya E, D'Agostino CA, Benayed R, Thomas RM. Extra-osseous Ewing sarcoma of the pancreas: case report with radiologic, pathologic, and molecular correlation, and brief review of the literature. Virchows Arch 2018 Sep;473(3):361-369.

(24) Dedeurwaerdere F, Giannini C, Sciot R, Rubin BP, Perilongo G, Borghi L, et al. Primary peripheral PNET/Ewing's sarcoma of the dura: a clinicopathologic entity distinct from central PNET. Mod Pathol 2002 Jun;15(6):673-678.

(25) Hasegawa SL, Davison JM, Rutten A, Fletcher JA, Fletcher CD. Primary cutaneous Ewing's sarcoma: immunophenotypic and molecular cytogenetic evaluation of five cases. Am J Surg Pathol 1998 Mar;22(3):310-318.

(26) Aurias A, Rimbaut C, Buffe D, Zucker JM, Mazabraud A. Translocation involving chromosome 22 in Ewing's sarcoma. A cytogenetic study of four fresh tumors. Cancer Genet Cytogenet 1984 May;12(1):21-25.

(27) Russell-Goldman E, Hornick JL, Qian X, Jo VY. NKX2.2 immunohistochemistry in the distinction of Ewing sarcoma from cytomorphologic mimics: Diagnostic utility and pitfalls. Cancer Cytopathol 2018 Nov;126(11):942-949.

(28) Ewing sarcoma and Ewing-like tumors.

(29) Antonescu CR, Owosho AA, Zhang L, Chen S, Deniz K, Huryn JM, et al. Sarcomas With CIC-rearrangements Are a Distinct Pathologic Entity With Aggressive Outcome: A Clinicopathologic and Molecular Study of 115 Cases. Am J Surg Pathol 2017 Jul;41(7):941-949.

(30) Casali PG, Bielack S, Abecassis N, Aro HT, Bauer S, Biagini R, et al. Bone sarcomas: ESMO–PaedCan–EURACAN Clinical Practice Guidelines for diagnosis, treatment and follow-up†. Annals of Oncology 2018;29:iv79-iv95.

(31) Sbaraglia M, Bellan E, Dei Tos AP. The 2020 WHO Classification of Soft Tissue Tumours: news and perspectives. Pathologica 2021 Apr;113(2):70-84.

(32) Antonescu C. Round cell sarcomas beyond Ewing: emerging entities. Histopathology 2014 Jan;64(1):26-37.

(33) Koelsche C, Kriegsmann M, Kommoss FK, Stichel D, Kriegsmann K, Vokuhl C, et al. DNA methylation profiling distinguishes Ewing-like sarcoma with EWSR1–NFATc2 fusion from Ewing sarcoma. J Cancer Res Clin Oncol 2019;145:1273-1281.

(34) Sadri N, Barroeta J, Pack SD, Abdullaev Z, Chatterjee B, Puthiyaveettil R, et al. Malignant round cell tumor of bone with EWSR1-NFATC2 gene fusion. Virchows Arch 2014 Aug;465(2):233-239.

(35) Chougule A, Taylor MS, Nardi V, Chebib I, Cote GM, Choy E, et al. Spindle and Round Cell Sarcoma With EWSR1-PATZ1 Gene Fusion: A Sarcoma With Polyphenotypic Differentiation. Am J Surg Pathol 2019 Feb;43(2):220-228.

(36) Bridge JA, Sumegi J, Druta M, Bui MM, Henderson-Jackson E, Linos K, et al. Clinical, pathological, and genomic features of EWSR1-PATZ1 fusion sarcoma. Mod Pathol 2019 Nov;32(11):1593-1604.

(37) Sadri N, Barroeta J, Pack SD, Abdullaev Z, Chatterjee B, Puthiyaveettil R, et al. Malignant round cell tumor of bone with EWSR1-NFATC2 gene fusion. Virchows Arch 2014 Aug;465(2):233-239.

(38) Wang GY, Thomas DG, Davis JL, Ng T, Patel RM, Harms PW, et al. EWSR1-NFATC2 Translocation-associated Sarcoma Clinicopathologic Findings in a Rare Aggressive Primary Bone or Soft Tissue Tumor. Am J Surg Pathol 2019 Aug;43(8):1112-1122.

(39) Michal M, Rubin BP, Agaimy A, Kosemehmetoglu K, Rudzinski ER, Linos K, et al. EWSR1-PATZ1-rearranged sarcoma: a report of nine cases of spindle and round cell neoplasms with predilection for thoracoabdominal soft tissues and frequent expression of neural and skeletal muscle markers. Modern Pathology 2021;34(4):770-785.

(40) Pierron G, Tirode F, Lucchesi C, Reynaud S, Ballet S, Cohen-Gogo S, et al. A new subtype of bone sarcoma defined by BCOR-CCNB3 gene fusion. Nat Genet 2012 Mar 4;44(4):461-466.

(41) Kao Y, Owosho AA, Sung Y, Zhang L, Fujisawa Y, Lee J, et al. BCOR-CCNB3 Fusion Positive Sarcomas: A Clinicopathologic and Molecular Analysis of 36 Cases With Comparison to Morphologic Spectrum and Clinical Behavior of Other Round Cell Sarcomas. Am J Surg Pathol 2018 May;42(5):604-615.

(42) Specht K, Zhang L, Sung Y, Nucci M, Dry S, Vaiyapuri S, et al. Novel BCOR-MAML3 and ZC3H7B-BCOR Gene Fusions in Undifferentiated Small Blue Round Cell Sarcomas. Am J Surg Pathol 2016 Apr;40(4):433-442.

(43) Puls F, Niblett A, Marland G, Gaston CLL, Douis H, Mangham DC, et al. BCOR-CCNB3 (Ewing-like) sarcoma: a clinicopathologic analysis of 10 cases, in comparison with conventional Ewing sarcoma. Am J Surg Pathol 2014 Oct;38(10):1307-1318.

(44) WHO Classification of Tumours Editorial Board editor. Soft Tissue and Bone Tumours. 5th Edition, Volume 3 ed.; 2020.

(45) Antonescu CR, Owosho AA, Zhang L, Chen S, Deniz K, Huryn JM, et al. Sarcomas With CIC-rearrangements Are a Distinct Pathologic Entity With Aggressive Outcome: A Clinicopathologic and Molecular Study of 115 Cases. Am J Surg Pathol 2017 Jul;41(7):941-949.

(46) Miettinen M, Felisiak-Golabek A, Luiña Contreras A, Glod J, Kaplan RN, Killian JK, et al. New fusion sarcomas: histopathology and clinical significance of selected entities. Hum Pathol 2019 Apr;86:57-65.

(47) Brčić I, Brodowicz T, Cerroni L, Kashofer K, Serbanescu GL, Kasseroler MT, et al. Undifferentiated round cell sarcomas with CIC-DUX4 gene fusion: expanding the clinical spectrum. Pathology 2020 Feb;52(2):236-242.

(48) Tang S, Dodd LG. CIC-DUX4 sarcoma diagnosed by fine-needle aspiration cytology: A case report. Diagn Cytopathol 2018 Nov;46(11):958-963.

(49) Camille A, Anne-Sophie B, Cécile P, Severine BC, Gaelle P, Olivier D, et al. Sarcoma With CIC-DUX4 Gene Fusion: Case Report of Kidney Tumor Location in a 12-year-old Boy. Pediatr Dev Pathol 2018;21(4):406-410.

(50) Lehane F, Tsikleas G, Bettington A, Limarporn K, Wilkinson L, Lehane K. "Cyst" on the forearm of a 28-year-old female: Case report of a CIC-rearranged sarcoma. J Cutan Pathol 2019 Aug;46(8):599-602.

(51) Maejima E, Mitsui H, Ohnuma T, Oishi N, Odate T, Deguchi N, et al. Case of CIC-DUX4 sarcoma of the skin: Histological simulant of epithelioid angiosarcoma. J Dermatol 2021;48(12):e594-e595.

(52) CIC capicua transcriptional repressor [Homo sapiens (human)]. 21-Jun-202321; Available at: https://www.ncbi.nlm.nih.gov/gene/23152.

(53) Lee Y. Regulation and function of capicua in mammals. Exp Mol Med 2020;52(4):531-537.

(54) Tanaka M, Yoshimoto T, Nakamura T. A double-edged sword: The world according to Capicua in cancer. Cancer Sci 2017 Dec;108(12):2319-2325.

(55) PDQ Pediatric Treatment Editorial Board. PDQ Pediatric Treatment Editorial Board. Ewing Sarcoma and Undifferentiated Small Round Cell Sarcomas of Bone and Soft Tissue Treatment (PDQ®). 2023; Available at: https://www.ncbi.nlm.nih.gov/books/NBK66045/.

(56) Stephanie Walter, Vedran Franke, Nir Drayman, Emanuel Wyler, Savaş Tay, Markus Landthaler, et al. Herpesviral induction of germline transcription factor DUX4 is critical for viral gene expression. bioRxiv 2021:2021.03.24.436599.

(57) Le Gall L, Sidlauskaite E, Mariot V, Dumonceaux J. Therapeutic Strategies Targeting DUX4 in FSHD. J Clin Med 2020 Sep 7;9(9):2886. doi: 10.3390/jcm9092886.

(58) Kawamura-Saito M, Yamazaki Y, Kaneko K, Kawaguchi N, Kanda H, Mukai H, et al. Fusion between CIC and DUX4 up-regulates PEA3 family genes in Ewing-like sarcomas with t(4;19)(q35;q13) translocation. Hum Mol Genet 2006 Jul 1;15(13):2125-2137.

(59) Choi SH, Gearhart MD, Cui Z, Bosnakovski D, Kim M, Schennum N, et al. DUX4 recruits p300/CBP through its C-terminus and induces global H3K27 acetylation changes. Nucleic Acids Res 2016;44(11):5161-5173.

(60) Forés M, Simón-Carrasco L, Ajuria L, Samper N, González-Crespo S, Drosten M, et al. A new mode of DNA binding distinguishes Capicua from other HMG-box factors and explains its mutation patterns in cancer. PLoS Genet 2017 Mar 9;13(3):e1006622.

(61) Yang S, Liu L, Yan Y, Jiang L, Han S, Shen D, et al. CIC-NUTM1 Sarcomas Affecting the Spine: A Subset of CIC-Rearranged Sarcomas Commonly Present in the Axial Skeleton. Arch Pathol Lab Med 2021 Sep 15.

(62) Mangray S, Kelly DR, LeGuellec S, Fridman E, Aggarwal S, Shago M, et al. Clinicopathologic Features of a Series of Primary Renal CIC-rearranged Sarcomas With Comprehensive Molecular Analysis. Am J Surg Pathol 2018 Oct;42(10):1360-1369.

(63) Sugita S, Arai Y, Tonooka A, Hama N, Totoki Y, Fujii T, et al. A novel CIC-FOXO4 gene fusion in undifferentiated small round cell sarcoma: a genetically distinct variant of Ewing-like sarcoma. Am J Surg Pathol 2014 Nov;38(11):1571-1576.

(64) Huang SC, Zhang L, Sung YS, Chen CL, Kao YC, Agaram NP, et al. Recurrent CIC Gene Abnormalities in Angiosarcomas: A Molecular Study of 120 Cases With Concurrent Investigation of PLCG1, KDR, MYC, and FLT4 Gene Alterations. Am J Surg Pathol 2016 May;40(5):645-655.

(65) Patra SK. Dissecting lipid raft facilitated cell signaling pathways in cancer. Biochim Biophys Acta 2008 Apr;1785(2):182-206.

(66) Bernardes N, Fialho AM. Perturbing the Dynamics and Organization of Cell Membrane Components: A New Paradigm for Cancer-Targeted Therapies. Int J Mol Sci 2018 Dec

4;19(12):3871. doi: 10.3390/ijms19123871.

(67) Ríos-Marco P, Marco C, Gálvez X, Jiménez-López JM, Carrasco MP. Alkylphospholipids: An update on molecular mechanisms and clinical relevance. Biochim Biophys Acta Biomembr 2017 Sep;1859(9 Pt B):1657-1667.

(68) Zalba S, Ten Hagen TLM. Cell membrane modulation as adjuvant in cancer therapy. Cancer Treat Rev 2017 Jan;52:48-57.

(69) Kopecka J, Trouillas P, Gašparović AČ, Gazzano E, Assaraf YG, Riganti C. Phospholipids and cholesterol: Inducers of cancer multidrug resistance and therapeutic targets. Drug Resist Updat 2020 Mar;49:100670.

(70) Kawata S, Takaishi K, Nagase T, Ito N, Matsuda Y, Tamura S, et al. Increase in the active form of 3-hydroxy-3-methylglutaryl coenzyme A reductase in human hepatocellular carcinoma: possible mechanism for alteration of cholesterol biosynthesis. Cancer Res 1990;50(11):3270-3273.

(71) Harwood Jr HJ, Alvarez IM, Noyes WD, Stacpoole PW. In vivo regulation of human leukocyte 3-hydroxy-3-methylglutaryl coenzyme A reductase: increased enzyme protein concentration and catalytic efficiency in human leukemia and lymphoma. J Lipid Res 1991;32(8):1237-1252.

(72) Peetla C, Vijayaraghavalu S, Labhasetwar V. Biophysics of cell membrane lipids in cancer drug resistance: Implications for drug transport and drug delivery with nanoparticles. Adv Drug Deliv Rev 2013;65(13-14):1686-1698.

(73) Niero EL, Rocha-Sales B, Lauand C, Cortez BA, de Souza MM, Rezende-Teixeira P, et al. The multiple facets of drug resistance: one history, different approaches. Journal of Experimental & Clinical Cancer Research 2014;33(1):1-14.

(74) Taniguchi M, Okazaki T. Role of ceramide/sphingomyelin (SM) balance regulated through "SM cycle" in cancer. Cell Signal 2021;87:110119.

(75) Tan LT, Chan K, Pusparajah P, Lee W, Chuah L, Khan TM, et al. Targeting membrane lipid a potential cancer cure? Frontiers in pharmacology 2017;8:12.

(76) Chen CY, Ingram MF, Rosal PH, Graham TR. Role for Drs2p, a P-type ATPase and potential aminophospholipid translocase, in yeast late Golgi function. J Cell Biol 1999 Dec 13;147(6):1223-1236.

(77) Senchenkov A, Litvak DA, Cabot MC. Targeting ceramide metabolism—a strategy for overcoming drug resistance. J Natl Cancer Inst 2001;93(5):347-357.

(78) Lewis AC, Wallington-Beddoe CT, Powell JA, Pitson SM. Targeting sphingolipid metabolism as an approach for combination therapies in haematological malignancies. Cell Death Discovery 2018;4(1):72.

(79) Walther TC, Farese Jr RV. Lipid droplets and cellular lipid metabolism. Annu Rev Biochem

2012;81:687-714.

(80) Tauchi-Sato K, Ozeki S, Houjou T, Taguchi R, Fujimoto T. The surface of lipid droplets is a phospholipid monolayer with a unique Fatty Acid composition. J Biol Chem 2002 Nov 15;277(46):44507-44512.

(81) Bozza PT, Magalhães KG, Weller PF. Leukocyte lipid bodies—biogenesis and functions in inflammation. Biochimica et Biophysica Acta (BBA)-Molecular and Cell Biology of Lipids 2009;1791(6):540-551.

(82) Murphy DJ. The dynamic roles of intracellular lipid droplets: from archaea to mammals. Protoplasma 2012;249:541-585.

(83) Röhrig F, Schulze A. The multifaceted roles of fatty acid synthesis in cancer. Nature Reviews Cancer 2016;16(11):732-749.

(84) Accioly MT, Pacheco P, Maya-Monteiro CM, Carrossini N, Robbs BK, Oliveira SS, et al. Lipid bodies are reservoirs of cyclooxygenase-2 and sites of prostaglandin-E2 synthesis in colon cancer cells. Cancer Res 2008;68(6):1732-1740.

(85) Huang W, Li X, Liu J, Lin J, Chung LW. Activation of Androgen Receptor, Lipogenesis, and Oxidative Stress Converged by SREBP-1 Is Responsible for Regulating Growth and Progression of Prostate Cancer CellsSREBP-1 Promotes Prostate Cancer Growth and Progression. Molecular Cancer Research 2012;10(1):133-142.

(86) Yue S, Li J, Lee S, Lee HJ, Shao T, Song B, et al. Cholesteryl ester accumulation induced by PTEN loss and PI3K/AKT activation underlies human prostate cancer aggressiveness. Cell metabolism 2014;19(3):393-406.

(87) Audet-Walsh É, Vernier M, Yee T, Laflamme C, Li S, Chen Y, et al. SREBF1 Activity Is Regulated by an AR/mTOR Nuclear Axis in Prostate CancerLipid Metabolism Regulation by an AR/mTOR/SREBF1 Axis. Molecular Cancer Research 2018;16(9):1396-1405.

(88) Morrison SF, Nakamura K, Madden CJ. Central control of thermogenesis in mammals. Exp Physiol 2008;93(7):773-797.

(89) Li J, Gu D, Lee SS, Song B, Bandyopadhyay S, Chen S, et al. Abrogating cholesterol esterification suppresses growth and metastasis of pancreatic cancer. Oncogene 2016;35(50):6378-6388.

(90) Valli A, Rodriguez M, Moutsianas L, Fischer R, Fedele V, Huang H, et al. Hypoxia induces a lipogenic cancer cell phenotype via HIF1alpha-dependent and -independent pathways. Oncotarget 2015 Feb 10;6(4):1920-1941.

(91) Guri Y, Colombi M, Dazert E, Hindupur SK, Roszik J, Moes S, et al. mTORC2 promotes tumorigenesis via lipid synthesis. Cancer cell 2017;32(6):807-823. e12.

(92) Yu M, Wang H, Zhao J, Yuan Y, Wang C, Li J, et al. Expression of CIDE proteins in clear cell renal cell carcinoma and their prognostic significance. Mol Cell Biochem 2013;378:145-151.

(93) O'Malley J, Kumar R, Kuzmin AN, Pliss A, Yadav N, Balachandar S, et al. Lipid quantification by Raman microspectroscopy as a potential biomarker in prostate cancer. Cancer Lett 2017;397:52-60.

(94) Schlaepfer IR, Hitz CA, Gijón MA, Bergman BC, Eckel RH, Jacobsen BM. Progestin modulates the lipid profile and sensitivity of breast cancer cells to docetaxel. Mol Cell Endocrinol 2012;363(1-2):111-121.

(95) Ladanyi A, Mukherjee A, Kenny HA, Johnson A, Mitra AK, Sundaresan S, et al. Adipocyte-induced CD36 expression drives ovarian cancer progression and metastasis. Oncogene 2018;37(17):2285-2301.

(96) Pascual G, Avgustinova A, Mejetta S, Martín M, Castellanos A, Attolini CS, et al. Targeting metastasis-initiating cells through the fatty acid receptor CD36. Nature 2017;541(7635):41-45.

(97) Cotte AK, Aires V, Fredon M, Limagne E, Derangère V, Thibaudin M, et al. Lysophosphatidylcholine acyltransferase 2-mediated lipid droplet production supports colorectal cancer chemoresistance. Nature communications 2018;9(1):322.

(98) Mondal S, Roy D, Sarkar Bhattacharya S, Jin L, Jung D, Zhang S, et al. Therapeutic targeting of PFKFB3 with a novel glycolytic inhibitor PFK158 promotes lipophagy and chemosensitivity in gynecologic cancers. International journal of cancer 2019;144(1):178-189.

(99) Ding X, Zhang W, Li S, Yang H. The role of cholesterol metabolism in cancer. Am J Cancer Res 2019 Feb 1;9(2):219-227.

(100) Kopecka J, Trouillas P, Gašparović AČ, Gazzano E, Assaraf YG, Riganti C. Phospholipids and cholesterol: Inducers of cancer multidrug resistance and therapeutic targets. Drug Resist Updat 2020 Mar;49:100670.

(101) Gelsomino G, Corsetto PA, Campia I, Montorfano G, Kopecka J, Castella B, et al. Omega 3 fatty acids chemosensitize multidrug resistant colon cancer cells by down-regulating cholesterol synthesis and altering detergent resistant membranes composition. Molecular Cancer 2013;12(1):137.

(102) Greife A, Tukova J, Steinhoff C, Scott SD, Schulz WA, Hatina J. Establishment and characterization of a bladder cancer cell line with enhanced doxorubicin resistance by mevalonate pathway activation. Tumor Biol 2015;36:3293-3300.

(103) Riganti C, Castella B, Kopecka J, Campia I, Coscia M, Pescarmona G, et al. Zoledronic acid restores doxorubicin chemosensitivity and immunogenic cell death in multidrug-resistant human cancer cells. PloS one 2013;8(4):e60975.

(104) Salaroglio IC, Campia I, Kopecka J, Gazzano E, Orecchia S, Ghigo D, et al. Zoledronic acid

overcomes chemoresistance and immunosuppression of malignant mesothelioma. Oncotarget 2015 Jan 20;6(2):1128-1142.

(105) Kopecka J, Porto S, Lusa S, Gazzano E, Salzano G, Giordano A, et al. Self-assembling nanoparticles encapsulating zoledronic acid revert multidrug resistance in cancer cells. Oncotarget 2015 Oct 13;6(31):31461-31478.

(106) Kopecka J, Porto S, Lusa S, Gazzano E, Salzano G, Pinzon-Daza ML, et al. Zoledronic acid-encapsulating self-assembling nanoparticles and doxorubicin: a combinatorial approach to overcome simultaneously chemoresistance and immunoresistance in breast tumors. Oncotarget 2016 Apr 12;7(15):20753-20772.

(107) Lin S, May EWS, Chang J, Hu R, Wang LH, Chan H. PGRMC1 contributes to doxorubicin-induced chemoresistance in MES-SA uterine sarcoma. Cellular and molecular life sciences 2015;72:2395-2409.

(108) Guéraud F, Atalay M, Bresgen N, Cipak A, Eckl PM, Huc L, et al. Chemistry and biochemistry of lipid peroxidation products. Free Radic Res 2010;44(10):1098-1124.

(109) Gasparovic AC, Milkovic L, Sunjic SB, Zarkovic N. Cancer growth regulation by 4-hydroxynonenal. Free Radical Biology and Medicine 2017;111:226-234.

(110) Camarillo JM, Ullery JC, Rose KL, Marnett LJ. Electrophilic modification of PKM2 by 4-hydroxynonenal and 4-oxononenal results in protein cross-linking and kinase inhibition. Chem Res Toxicol 2017;30(2):635-641.

(111) Castro JP, Jung T, Grune T, Siems W. 4-Hydroxynonenal (HNE) modified proteins in metabolic diseases. Free Radical Biology and Medicine 2017;111:309-315.

(112) Jovanovic O, Pashkovskaya AA, Annibal A, Vazdar M, Burchardt N, Sansone A, et al. The molecular mechanism behind reactive aldehyde action on transmembrane translocations of proton and potassium ions. Free Radical Biology and Medicine 2015;89:1067-1076.

(113) Jovanović O, Škulj S, Pohl EE, Vazdar M. Covalent modification of phosphatidylethanolamine by 4-hydroxy-2-nonenal increases sodium permeability across phospholipid bilayer membranes. Free Radical Biology and Medicine 2019;143:433-440.

(114) Laurora S, Tamagno E, Briatore F, Bardini P, Pizzimenti S, Toaldo C, et al. 4-Hydroxynonenal modulation of p53 family gene expression in the SK-N-BE neuroblastoma cell line. Free Radical Biology and Medicine 2005;38(2):215-225.

(115) Milkovic L, Cipak Gasparovic A, Zarkovic N. Overview on major lipid peroxidation bioactive factor 4-hydroxynonenal as pluripotent growth-regulating factor. Free Radic Res 2015;49(7):850-860.

(116) Mol M, Regazzoni L, Altomare A, Degani G, Carini M, Vistoli G, et al. Enzymatic and non-enzymatic detoxification of 4-hydroxynonenal: Methodological aspects and biological

consequences. Free Radical Biology and Medicine 2017;111:328-344.

(117) Muzio G, Ricci M, Traverso N, Monacelli F, Oraldi M, Maggiora M, et al. 4-Hydroxyhexenal and 4-hydroxynonenal are mediators of the anti-cachectic effect of n-3 and n-6 polyunsaturated fatty acids on human lung cancer cells. Free Radical Biology and Medicine 2016;99:63-70.

(118) Shoeb M, H Ansari N, K Srivastava S, V Ramana K. 4-Hydroxynonenal in the pathogenesis and progression of human diseases. Curr Med Chem 2014;21(2):230-237.

(119) Singhal SS, Singh SP, Singhal P, Horne D, Singhal J, Awasthi S. Antioxidant role of glutathione S-transferases: 4-Hydroxynonenal, a key molecule in stress-mediated signaling. Toxicol Appl Pharmacol 2015;289(3):361-370.

(120) Vazdar K, Vojta D, Margetic D, Vazdar M. Reaction mechanism of covalent modification of phosphatidylethanolamine lipids by reactive aldehydes 4-hydroxy-2-nonenal and 4-oxo-2-nonenal. Chem Res Toxicol 2017;30(3):840-850.

(121) Zarkovic N, Ilic Z, Jurin M, Schaur RJ, Puhl H, Esterbauer H. Stimulation of HeLa cell growth by physiological concentrations of 4-hydroxynonenal. Cell Biochemistry and Function: Cellular biochemistry and its modulation by active agents or disease 1993;11(4):279-286.

(122) Zhang H, Forman HJ. 4-hydroxynonenal-mediated signaling and aging. Free Radical Biology and Medicine 2017;111:219-225.

(123) Zimmermann L, Moldzio R, Vazdar K, Krewenka C, Pohl EE. Nutrient deprivation in neuroblastoma cells alters 4-hydroxynonenal-induced stress response. Oncotarget 2017 Jan 31;8(5):8173-8188.

(124) Kopecka J, Trouillas P, Gašparović AČ, Gazzano E, Assaraf YG, Riganti C. Phospholipids and cholesterol: Inducers of cancer multidrug resistance and therapeutic targets. Drug Resistance Updates 2020;49:100670.

(125) El-Kenawi A, Ruffell B. Inflammation, ROS, and mutagenesis. Cancer cell 2017;32(6):727-729.

(126) Milkovic L, Zarkovic N, Saso L. Controversy about pharmacological modulation of Nrf2 for cancer therapy. Redox biology 2017;12:727-732.

(127) Ishikado A, Morino K, Nishio Y, Nakagawa F, Mukose A, Sono Y, et al. 4-Hydroxy hexenal derived from docosahexaenoic acid protects endothelial cells via Nrf2 activation. PloS one 2013;8(7):e69415.

(128) Venkatraman G, Benesch MG, Tang X, Dewald J, McMullen TP, Brindley DN. Lysophosphatidate signaling stabilizes Nrf2 and increases the expression of genes involved in drug resistance and oxidative stress responses: implications for cancer treatment. The FASEB Journal 2015;29(3):772-785.

(129) Lin S, May EWS, Chang J, Hu R, Wang LH, Chan H. PGRMC1 contributes to doxorubicin-induced chemoresistance in MES-SA uterine sarcoma. Cellular and molecular life sciences 2015;72:2395-2409.

(130) Shen S, Yang L, Li L, Bai Y, Cai C, Liu H. A plasma lipidomics strategy reveals perturbed lipid metabolic pathways and potential lipid biomarkers of human colorectal cancer. Journal of Chromatography B 2017;1068:41-48.

(131) Lin H, Mahon KL, Weir JM, Mundra PA, Spielman C, Briscoe K, et al. A distinct plasma lipid signature associated with poor prognosis in castration-resistant prostate cancer. International Journal of Cancer 2017;141(10):2112-2120.

(132) Ide Y, Waki M, Hayasaka T, Nishio T, Morita Y, Tanaka H, et al. Human breast cancer tissues contain abundant phosphatidylcholine (36∶ 1) with high stearoyl-CoA desaturase-1 expression. PloS one 2013;8(4):e61204.

(133) Melis Kartal Yandım, Elif Apohan & Yusuf Baran. Therapeutic potential of targeting ceramide/glucosylceramide pathway in cancer. 2012(- 1532-2084 (Electronic); - 1368-7646 (Linking)).

(134) FU Berlin. http://webdoc.sub.gwdg.de/ebook/diss/2003/fu-berlin/2002/180/Einleitung.pdf. 2003.

(135) Liu YY, Hill RA, Li YT. Ceramide glycosylation catalyzed by glucosylceramide synthase and cancer drug resistance. Adv Cancer Res 2013;117:59-89.

(136) Chai L, McLaren RP, Byrne A, Chuang WL, Huang Y, Dufault MR, et al. The chemosensitizing activity of inhibitors of glucosylceramide synthase is mediated primarily through modulation of P-gp function. Int J Oncol 2011 Mar;38(3):701-711.

(137) Gouazé V, Yu JY, Bleicher RJ, Han TY, Liu YY, Wang H, et al. Overexpression of glucosylceramide synthase and P-glycoprotein in cancer cells selected for resistance to natural product chemotherapy. Mol Cancer Ther 2004 May;3(5):633-639.

(138) Hartwig P, Höglinger D. The Glucosylceramide Synthase Inhibitor PDMP Causes Lysosomal Lipid Accumulation and mTOR Inactivation. Int J Mol Sci 2021 Jun 30;22(13):7065. doi: 10.3390/ijms22137065.

(139) Chatterjee S, Alsaeedi N, Hou J, Bandaru VV, Wu L, Halushka MK, et al. Use of a glycolipid inhibitor to ameliorate renal cancer in a mouse model. PLoS One 2013 May 9;8(5):e63726.

(140) Koike K, Berdyshev EV, Mikosz AM, Bronova IA, Bronoff AS, Jung JP, et al. Role of Glucosylceramide in Lung Endothelial Cell Fate and Emphysema. Am J Respir Crit Care Med 2019 Nov 1;200(9):1113-1125.

(141) Xie P, Shen YF, Shi YP, Ge SM, Gu ZH, Wang J, et al. Overexpression of glucosylceramide synthase in associated with multidrug resistance of leukemia cells. Leuk Res 2008 Mar;32(3):475-

480.

(142) Gouazé V, Yu JY, Bleicher RJ, Han TY, Liu YY, Wang H, et al. Overexpression of glucosylceramide synthase and P-glycoprotein in cancer cells selected for resistance to natural product chemotherapy. Mol Cancer Ther 2004 May;3(5):633-639.

(143) Shen W, Henry AG, Paumier KL, Li L, Mou K, Dunlop J, et al. Inhibition of glucosylceramide synthase stimulates autophagy flux in neurons. J Neurochem 2014 Jun;129(5):884-894.

(144) Murugan AK. mTOR: Role in cancer, metastasis and drug resistance. Semin Cancer Biol 2019 Dec;59:92-111.

(145) Hua H, Kong Q, Zhang H, Wang J, Luo T, Jiang Y. Targeting mTOR for cancer therapy. J Hematol Oncol 2019 Jul 5;12(1):71-1.

(146) Guri Y, Colombi M, Dazert E, Hindupur SK, Roszik J, Moes S, et al. mTORC2 Promotes Tumorigenesis via Lipid Synthesis. Cancer Cell 2017;32(6):807-823.e12.

(147) Guri Y, Colombi M, Dazert E, Hindupur SK, Roszik J, Moes S, et al. mTORC2 Promotes Tumorigenesis via Lipid Synthesis. Cancer Cell 2017 Dec 11;32(6):807-823.e12.

(148) Kuemmerle NB, Rysman E, Lombardo PS, Flanagan AJ, Lipe BC, Wells WA, et al. Lipoprotein lipase links dietary fat to solid tumor cell proliferation. Molecular cancer therapeutics 2011;10(3):427-436.

(149) Zaidi N, Lupien L, Kuemmerle NB, Kinlaw WB, Swinnen JV, Smans K. Lipogenesis and lipolysis: the pathways exploited by the cancer cells to acquire fatty acids. Prog Lipid Res 2013;52(4):585-589.

(150) Munir R, Lisec J, Swinnen JV, Zaidi N. Lipid metabolism in cancer cells under metabolic stress. Br J Cancer 2019 Jun;120(12):1090-1098.

(151) Sim J, Cowburn AS, Palazon A, Madhu B, Tyrakis PA, Macías D, et al. The Factor Inhibiting HIF Asparaginyl Hydroxylase Regulates Oxidative Metabolism and Accelerates Metabolic Adaptation to Hypoxia. Cell Metabolism 2018;27(4):898-913.e7.

(152) Li H, Zhou Y, Li L, Li S, Long D, Chen X, et al. HIF-1α protects against oxidative stress by directly targeting mitochondria. Redox Biology 2019;25:101109.

(153) Yang G, Shi R, Zhang Q. Hypoxia and Oxygen-Sensing Signaling in Gene Regulation and Cancer Progression. Int J Mol Sci 2020 Oct 31;21(21):8162. doi: 10.3390/ijms21218162.

(154) Brown LM, Cowen RL, Debray C, Eustace A, Erler JT, Sheppard FCD, et al. Reversing hypoxic cell chemoresistance in vitro using genetic and small molecule approaches targeting hypoxia inducible factor-1. Mol Pharmacol 2006 Feb;69(2):411-418.

(155) Hao J, Song X, Song B, Liu Y, Wei L, Wang X, et al. Effects of lentivirus-mediated HIF-1alpha knockdown on hypoxia-related cisplatin resistance and their dependence on p53 status in fibrosarcoma cells. Cancer Gene Ther 2008 Jul;15(7):449-455.

(156) Liu Y, Veena CK, Morgan JB, Mohammed KA, Jekabsons MB, Nagle DG, et al. Methylalpinumisoflavone inhibits hypoxia-inducible factor-1 (HIF-1) activation by simultaneously targeting multiple pathways. J Biol Chem 2009 Feb 27;284(9):5859-5868.

(157) Nardinocchi L, Puca R, Sacchi A, D'Orazi G. Inhibition of HIF-1alpha activity by homeodomain-interacting protein kinase-2 correlates with sensitization of chemoresistant cells to undergo apoptosis. Mol Cancer 2009 Jan 7;8:1-1.

(158) Nardinocchi L, Puca R, Sacchi A, Rechavi G, Givol D, D'Orazi G. Targeting hypoxia in cancer cells by restoring homeodomain interacting protein-kinase 2 and p53 activity and suppressing HIF-1alpha. PLoS One 2009 Aug 28;4(8):e6819.

(159) Nardinocchi L, Puca R, Guidolin D, Belloni AS, Bossi G, Michiels C, et al. Transcriptional regulation of hypoxia-inducible factor 1alpha by HIPK2 suggests a novel mechanism to restrain tumor growth. Biochim Biophys Acta 2009 Feb;1793(2):368-377.

(160) Sasabe E, Zhou X, Li D, Oku N, Yamamoto T, Osaki T. The involvement of hypoxia-inducible factor-1alpha in the susceptibility to gamma-rays and chemotherapeutic drugs of oral squamous cell carcinoma cells. Int J Cancer 2007 Jan 15;120(2):268-277.

(161) Sullivan R, Graham CH. Chemosensitization of cancer by nitric oxide. Curr Pharm Des 2008;14(11):1113-1123.

(162) Sullivan R, Paré GC, Frederiksen LJ, Semenza GL, Graham CH. Hypoxia-induced resistance to anticancer drugs is associated with decreased senescence and requires hypoxia-inducible factor-1 activity. Mol Cancer Ther 2008 Jul;7(7):1961-1973.

(163) Chang Q, Qin R, Huang T, Gao J, Feng Y. Effect of antisense hypoxia-inducible factor 1alpha on progression, metastasis, and chemosensitivity of pancreatic cancer. Pancreas 2006 Apr;32(3):297-305.

(164) Chang C, Lin M, Lin B, Jeng Y, Chen S, Chu C, et al. Effect of connective tissue growth factor on hypoxia-inducible factor 1alpha degradation and tumor angiogenesis. J Natl Cancer Inst 2006 Jul 19;98(14):984-995.

(165) Hussein D, Estlin EJ, Dive C, Makin GWJ. Chronic hypoxia promotes hypoxia-inducible factor-1alpha-dependent resistance to etoposide and vincristine in neuroblastoma cells. Mol Cancer Ther 2006 Sep;5(9):2241-2250.

(166) Li QF, Wang XR, Yang YW, Lin H. Hypoxia upregulates hypoxia inducible factor (HIF)-3alpha expression in lung epithelial cells: characterization and comparison with HIF-1alpha. Cell Res 2006 Jun;16(6):548-558.

(167) Li L, Lin X, Shoemaker AR, Albert DH, Fesik SW, Shen Y. Hypoxia-inducible factor-1 inhibition in combination with temozolomide treatment exhibits robust antitumor efficacy in vivo. Clin Cancer Res 2006 Aug 1;12(15):4747-4754.

(168) Rohwer N, Dame C, Haugstetter A, Wiedenmann B, Detjen K, Schmitt CA, et al. Hypoxia-inducible factor 1alpha determines gastric cancer chemosensitivity via modulation of p53 and NF-kappaB. PLoS One 2010 Aug 10;5(8):e12038.

(169) Evens AM, Sehn LH, Farinha P, Nelson BP, Raji A, Lu Y, et al. Hypoxia-inducible factor-1 {alpha} expression predicts superior survival in patients with diffuse large B-cell lymphoma treated with R-CHOP. J Clin Oncol 2010 Feb 20;28(6):1017-1024.

(170) Cellosaurus. No title. 2022; Available at: https://www.cellosaurus.org/CVCL_1411.

(171) Graham K, Unger E. Overcoming tumor hypoxia as a barrier to radiotherapy, chemotherapy and immunotherapy in cancer treatment. International journal of nanomedicine 2018;13:6049-6058.

(172) Matyash V, Liebisch G, Kurzchalia TV, Shevchenko A, Schwudke D. Lipid extraction by methyl-tert-butyl ether for high-throughput lipidomics. J Lipid Res 2008 May;49(5):1137-1146.

(173) Triebl A, Hartler J, Trötzmüller M, C Köfeler H. Lipidomics: Prospects from a technological perspective. Biochim Biophys Acta Mol Cell Biol Lipids 2017 Aug;1862(8):740-746.

(174) Hartler J, Trötzmüller M, Chitraju C, Spener F, Köfeler HC, Thallinger GG. Lipid Data Analyzer: unattended identification and quantitation of lipids in LC-MS data. Bioinformatics 2011 Feb 15;27(4):572-577.

(175) Hartler J, Triebl A, Ziegl A, Trötzmüller M, Rechberger GN, Zeleznik OA, et al. Deciphering lipid structures based on platform-independent decision rules. Nature Methods 2017;14(12):1171-1174.

(176) McGrail DJ, Pilié PG, Rashid NU, Voorwerk L, Slagter M, Kok M, et al. High tumor mutation burden fails to predict immune checkpoint blockade response across all cancer types. Annals of Oncology 2021;32(5):661-672.

(177) Choi M, Kipps T, Kurzrock R. ATM Mutations in Cancer: Therapeutic Implications. Mol Cancer Ther 2016 Aug;15(8):1781-1791.

(178) Klempner SJ, Fabrizio D, Bane S, Reinhart M, Peoples T, Ali SM, et al. Tumor Mutational Burden as a Predictive Biomarker for Response to Immune Checkpoint Inhibitors: A Review of Current Evidence. Oncologist 2020 Jan;25(1):e147-e159.

(179) Connolly EA, Bhadri VA, Wake J, Ingley KM, Lewin J, Bae S, et al. Systemic treatments and outcomes in CIC-rearranged Sarcoma: A national multi-centre clinicopathological series and literature review. Cancer Med 2023;11(8):1805-1816.

(180) Yoshimoto T, Tanaka M, Homme M, Yamazaki Y, Takazawa Y, Antonescu CR, et al. CIC-DUX4 Induces Small Round Cell Sarcomas Distinct from Ewing Sarcoma. Cancer Res 2017 Jun 1;77(11):2927-2937.

(181) Rekhi B, Kembhavi P, Mishra SN, Shetty O, Bajpai J, Puri A. Clinicopathologic features of undifferentiated round cell sarcomas of bone & soft tissues: An attempt to unravel the BCOR-CCNB3- & CIC-DUX4-positive sarcomas. Indian J Med Res 2019;150(6):557-574.

(182) Chebib I, Jo VY. Round cell sarcoma with CIC-DUX4 gene fusion: Discussion of the distinctive cytomorphologic, immunohistochemical, and molecular features in the differential diagnosis of round cell tumors. Cancer Cytopathol 2016 May;124(5):350-361.

(183) Brennan B, Kirton L, Marec-Bérard P, Gaspar N, Laurence V, Martín-Broto J, et al. Comparison of two chemotherapy regimens in patients with newly diagnosed Ewing sarcoma (EE2012): an open-label, randomised, phase 3 trial. The Lancet 2022;400(10362):1513-1521.

(184) Oyama R, Takahashi M, Yoshida A, Sakumoto M, Takai Y, Kito F, et al. Generation of novel patient-derived CIC- DUX4 sarcoma xenografts and cell lines. Sci Rep 2017 Jul 5;7(1):4712-0.

(185) Hesla AC, Papakonstantinou A, Tsagkozis P. Current Status of Management and Outcome for Patients with Ewing Sarcoma. Cancers (Basel) 2021 Mar 10;13(6):1202. doi: 10.3390/cancers13061202.

(186) Yang R, Yi M, Xiang B. Novel Insights on Lipid Metabolism Alterations in Drug Resistance in Cancer. Front Cell Dev Biol 2022 May 13;10:875318.

(187) Li Y, Zhao L, Li X. Hypoxia and the Tumor Microenvironment. Technol Cancer Res Treat 2021;20:15330338211036304.

(188) Yosef HK, Mavarani L, Maghnouj A, Hahn S, El-Mashtoly SF, Gerwert K. In vitro prediction of the efficacy of molecularly targeted cancer therapy by Raman spectral imaging. Anal Bioanal Chem 2015 Nov;407(27):8321-8331.

(189) Verbrugge SE, Al M, Assaraf YG, Kammerer S, Chandrupatla DMSH, Honeywell R, et al. Multifactorial resistance to aminopeptidase inhibitor prodrug CHR2863 in myeloid leukemia cells: down-regulation of carboxylesterase 1, drug sequestration in lipid droplets and pro-survival activation ERK/Akt/mTOR. Oncotarget 2016;7(5):5240.

(190) Schlaepfer IR, Hitz CA, Gijón MA, Bergman BC, Eckel RH, Jacobsen BM. Progestin modulates the lipid profile and sensitivity of breast cancer cells to docetaxel. Mol Cell Endocrinol 2012 Nov 5;363(1-2):111-121.

(191) Englinger B, Laemmerer A, Moser P, Kallus S, Röhrl C, Pirker C, et al. Lipid droplet-mediated scavenging as novel intrinsic and adaptive resistance factor against the multikinase inhibitor ponatinib. International journal of cancer 2020;147(6):1680-1693.

(192) Cheng M, Bhujwalla ZM, Glunde K. Targeting Phospholipid Metabolism in Cancer. Front

Oncol 2016 Dec 27;6:266.

(193) Uta Dirksen, Thomas Brodowicz, Jendrik Hardes, Wolfgang Hartmann, Yvonne Hummel, Peter Reichardt, Beate Timmermann. Ewing Sarkom. 2020; Available at: https://www.onkopedia.com/de/onkopedia/guidelines/ewing-sarkom/@@guideline/html/index.html. Accessed 03., 2023.

Appendix

Data Collection Sheet						
	Project / Institute	Rinner		←		*dark fields are filled in by the customer !*
	Name (contact person)	Florian Zemljic			operator:	VB
	Phone. Nr.	66[redacted]			Project ID:	MS 21-008
	email	florian.zemljic@stud.medunigraz.at			date of receipt:	17.03.2021
	sample return after analysis		no		requested analyte (method):	Lipidprofile
	note: stored samples will be discarded after 6 months !				storage of the samples in the lab:	-80 °C
					date of sample return, sign:	

internal number	sample name or number (= tube name) min. 3 letters!!	material (Sarcoma cells)	quantity (cellnumber)	proceeding before sample delivery (lipid extraction e.g. MTBE, Bligh&Dyer)	sample storage before delivery	note
1	1	MHH-Es-1 - FBS - Hypoxia (1,5% o2)	1,00E+06	to stop encymatic degradation -> 1ml Meoh given	4°C	
2	2	MHH-Es-1 - FBS - Hypoxia (1,5% o2)	1,00E+06	to stop encymatic degradation -> 1ml Meoh given	4°C	
3	3	MHH-Es-1 - FBS - Hypoxia (1,5% o2)	1,00E+06	to stop encymatic degradation -> 1ml Meoh given	4°C	
4	4	MHH-Es-1 - FBS - Hypoxia (1,5% o2)	1,00E+06	to stop encymatic degradation -> 1ml Meoh given	4°C	
5	5	MHH-Es-1 - FBS - Hypoxia (1,5% o2)	1,00E+06	to stop encymatic degradation -> 1ml Meoh given	4°C	
6	6	MUG CIDUS - FBS - Hypoxia (1,5%)	1,00E+06	to stop encymatic degradation -> 1ml Meoh given	4°C	
7	7	MUG CIDUS - FBS - Hypoxia (1,5%)	1,00E+06	to stop encymatic degradation -> 1ml Meoh given	4°C	
8	8	MUG CIDUS - FBS - Hypoxia (1,5%)	1,00E+06	to stop encymatic degradation -> 1ml Meoh given	4°C	
9	9	MUG CIDUS - FBS - Hypoxia (1,5%)	1,00E+06	to stop encymatic degradation -> 1ml Meoh given	4°C	
10	10	MUG CIDUS - FBS - Hypoxia (1,5%)	1,00E+06	to stop encymatic degradation -> 1ml Meoh given	4°C	
16	16	MHH-Es-1 - FBS - Normoxia	1,00E+06	to stop encymatic degradation -> 1ml Meoh given	4°C	
17	17	MHH-Es-1 - FBS - Normoxia	1,00E+06	to stop encymatic degradation -> 1ml Meoh given	4°C	
18	18	MHH-Es-1 - FBS - Normoxia	1,00E+06	to stop encymatic degradation -> 1ml Meoh given	4°C	
19	19	MHH-Es-1 - FBS - Normoxia	1,00E+06	to stop encymatic degradation -> 1ml Meoh given	4°C	
20	20	MHH-Es-1 - FBS - Normoxia	1,00E+06	to stop encymatic degradation -> 1ml Meoh given	4°C	
21	21	MUG CIDUS- FBS -Normoxia	1,00E+06	to stop encymatic degradation -> 1ml Meoh given	4°C	
22	22	MUG CIDUS- FBS -Normoxia	1,00E+06	to stop encymatic degradation -> 1ml Meoh given	4°C	
23	23	MUG CIDUS- FBS -Normoxia	1,00E+06	to stop encymatic degradation -> 1ml Meoh given	4°C	
24	24	MUG CIDUS- FBS -Normoxia	1,00E+06	to stop encymatic degradation -> 1ml Meoh given	4°C	
25	25	MUG CIDUS- FBS -Normoxia	1,00E+06	to stop encymatic degradation -> 1ml Meoh given	4°C	

Table 1, List of samples for the lipidomic